

AIRBORNE RADAR GROUND CLUTTER
RETURN

by

ROBERT A. McMILLEN

B. S., Kansas State University, 1960

A MASTER'S THESIS

submitted in partial fulfillment of the

requirements for the degree

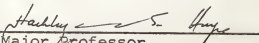
MASTER OF SCIENCE

Department of Electrical Engineering

KANSAS STATE UNIVERSITY
Manhattan, Kansas

1964

Approved by:


Major Professor

LD
2668
T4
1964
M16
C.2
Document

TABLE OF CONTENTS

INTRODUCTION	1
BASIC RADAR RETURN THEORY	2
The Basic Radar	2
Electromagnetic Wave Scattering From Terrain	3
SIGNAL CORRELATION AND POWER SPECTRUM	6
CLUTTER MODELS AND POWER SPECTRUM CALCULATIONS	9
Random Models	12
Deterministic Models	26
MATHEMATICAL MODEL FOR GROUND CLUTTER POWER SPECTRUM FOR AN AIRBORNE PULSE RADAR	41
Clutter Geometry	41
Calculation of Received Power	46
CALCULATED POWER SPECTRUMS	53
Incremental Areas	53
Scattering Coefficients	54
Antenna Pattern	56
Altitude and Power	57
Power Spectrum	57
Results	58
SUMMARY	63
ACKNOWLEDGMENTS	66
REFERENCES	67
APPENDIX	69

INTRODUCTION

The basic design criterion of a radar target detection system is to detect the desired target signal in the presence of undesired signals. In the class of radars called airborne moving target indicators, (AMTI), the desired target is an aircraft and the undesired signal is the return from the ground or other stationary objects. This ground return is commonly called "clutter".

There are two basic methods used in the design of AMTI systems, namely, doppler frequency detection and clutter cancellation by correlation methods. The former is a frequency filtering technique whereas the latter is a time domain technique. Both methods encounter severe limitations when the range rate is such that the target return spectrum is in the same frequency range as the clutter return spectrum. In this case the target signal is superimposed with strong clutter signal. In order to separate the target from the clutter under this condition, one needs to correlate the characteristics of the target return, and those of the clutter, and thus extracting the target information.

In the analysis and design of the AMTI radar, it is necessary to establish an accurate model of the clutter return. First the methods of analysis and the clutter models reported in the literature are discussed. Then a modified mathematical model is proposed and its details are given. The effect of terrain roughness on the clutter spectrum given by the model was calculated using the IBM 1620 computer. The Hayre-Moore (1962)

derivation for the scattering coefficient plays a central role in this analysis.

BASIC RADAR RETURN THEORY

The Basic Radar

A radar is an electronic device for detection and location of targets by transmitting an electromagnetic signal and detecting the reflected return signal. An elementary radar consists of a transmitter to generate the signal, an antenna to radiate the outgoing signal and collect the incoming signal, and a receiver to detect and process the return signal.

The range to the target is measured by the time required for the incident signal to reach the target and the reflected signal to arrive back at the radar. If there is relative motion between the radar and the target, the shift in the carrier frequency of the reflected wave (doppler shift) is a measure of the target's relative velocity. This property distinguishes moving targets from stationary objects. The distance or range, R , to the target is

$$R = \frac{c\Delta t}{2} \quad (1)$$

where

$c = 3 \times 10^8$ meters/second (velocity of light)

Δt = time required for the wave to travel out and back.

The received power, P_r , of the return signal from a point source is given by the radar equation

$$P_r = \frac{P_t G^2 \lambda^2 \sigma_o'}{(4\pi)^3 R^4} \quad (2)$$

where

P_t = power transmitted

G = antenna gain

λ = wavelength

σ_o' = radar cross-section

This basic expression is a simplified form and does not adequately describe the performance of a practical radar because the parameters in general are variable functions.

Electromagnetic Wave Scattering From Terrain

(Hayre and Moore, 1962)

Electromagnetic waves are reflected, refracted, and absorbed by media present in their propagation path, depending on the properties of the media. Some of the energy of such incident waves is deflected away from the original direction of propagation. Energy deflected back toward the source is called backscatter and energy deflected away from the source is called forward scatter.

Surface scattering is the scattering of the incident wave in various directions by the surface irregularities. A complete solution for scattering from randomly rough surfaces is not yet known, although a great many approximations have been attempted. This type of scattering is of primary concern in this paper since clutter is the return signal from a rough surface.

Hayre (1962) has developed a model for the radar scattering

cross-section per unit area (σ_0) of a rough surface, based on statistical parameters of the terrain. Scattering phenomenon is measured by the radar scattering cross-section per unit area, where

$$\sigma_0 = \lim_{R \rightarrow \infty} 4\pi R^2 \left| \frac{E_R^S}{E_i^2} \right|^2 \quad (3)$$

and

E_R^S = scattered electric field at the receiving antenna

E_i = incident plane wave field.

The total radar scattering cross-section is obtained by integrating σ_0 over the target surface. The average power received from the target surface is

$$\bar{P}_R = \frac{\lambda^2}{32\pi^2} \iint P_T \left(T - \frac{2R}{C}\right) G^2(\theta, \phi) \sigma_0(\theta, \lambda) \frac{1}{R^3} dR d\phi \quad (4)$$

where

\bar{P}_R = average power received

T = delay time measured from the start of the transmitted pulse

ϕ = angle in the ground plane from antenna boresight to the target

θ = angle of incidence measured outward from the surface normal.

The radar scattering cross-section is assumed to be independent of ϕ . This equation forms the basis of a model used in this analysis.

The Hayre and Moore (1962) scattering coefficient is based

on statistical parameters determined from contour map data. Their results were used to calculate scattering coefficients for comparison with experimental data. It has been shown that the normalized values of σ_0 compare very closely with both experimental values, and the results of acoustical simulation. Their scattering coefficient is given as

$$\sigma_0 = \frac{4\sqrt{2}\pi B^2}{\lambda^2} \left(\frac{\sigma}{\sin\theta}\right) \exp\{-4k^2\sigma^2\cos^2\theta\} \chi \sum_{n=1}^{\infty} \frac{(4k^2\sigma^2)^n (\cos^2\theta)^{n+1}}{(n-1)! (2k^2 B^2 \sin^2\theta + n^2)^{3/2}} \quad (5)$$

where

B = characteristic constant determined from the surface roughness autocovariance function $\rho(r)$

σ = standard deviation of the target terrain heights about the mean

k = wavenumber ($2\pi/\lambda$)

$\rho(r)$ = $\exp(-|r|/B)$ normalized space-height autocorrelation function

r = distance between points on the surface.

For values of $1/B$ small as compared to k , the above expression becomes

$$\sigma_0 = \frac{4\sigma^2}{\lambda B} (\theta \cot^4 \theta) \text{ for } \theta \neq 0^\circ \quad (6)$$

The scattering coefficient listed in Equation (5) shows the effect of small scale surface roughness on the radar return. The increasing value of B/λ indicates increasing horizontal roughness. The value σ/λ indicates the relative small scale

vertical terrain heights. (Hayre and Moore, 1962)

SIGNAL CORRELATION AND POWER SPECTRUM

A basic technique used in the detection of signals in the presence of noise is correlation of the return signal and a reference signal. If the reference signal is the return signal delayed in time, then the process is called autocorrelation. If a signal other than the return signal is used as the reference, then the process is called cross-correlation. The basic relationship for the correlation functions and the power spectra are later derived using random variable theory.

One of the major problems in the analysis and design of radar systems, is that the signal return has random variations that must be described statistically. The main features of a random process, $x(t)$, are indeterminacy in the expected behavior of any single record, together with strong statistical properties of a collection (ensemble) of its records. A random process can then be defined as an ensemble of time functions $\{x_k(t)\}$, $-\infty < t < \infty$, $k = 1, 2, \dots$, such that the ensemble can be characterized by statistical properties. (Bendat, 1958)

There are two averages associated with a random process, namely the time average, and the ensemble average. The time average of a single record over the time interval is given by

$$\overline{x(t)} = \lim_{T \rightarrow \infty} \frac{1}{2T} \int_{-T}^T x(t) dt \quad (7)$$

The ensemble average is the average of all the records at a particular time t_1 , as given by

$$E[K_{x(t_1)}] = \int_{-\infty}^{\infty} K_x(t) p(x) dx \quad (8)$$

With this introduction to random processes, the relationship between correlation functions and power spectrum is derived (Lanning and Battin, 1956). First the autocorrelation function, $\phi_{xx}(t, t + \tau)$, is defined to be

$$\phi_{xx}(t, t + \tau) = E[x(t)x(t + \tau)] \quad (9)$$

It is desired to show that a relationship exists between the correlation function and the power spectra for any random process. We define a quantity $\psi_T(\tau)$ to be

$$\psi_T(\tau) = \frac{1}{2T} \int_{-\infty}^{\infty} x_T(t)x_T(t + \tau) dt \quad (10)$$

where $x_T(t)$ denotes a truncated time function. Next the quantity $\psi(\tau)$ is defined as

$$\psi(\tau) = \lim_{T \rightarrow \infty} \psi_T(\tau) = \lim_{T \rightarrow \infty} \frac{1}{2T} \int_{-T}^T x(t)x(t + \tau) dt \quad (11)$$

Taking the Fourier Transform of $\psi(\tau)$, one obtains

$$\frac{1}{\pi} \int_{-\infty}^{\infty} \psi(\tau) e^{-jw\tau} d\tau = \lim_{T \rightarrow \infty} \frac{1}{\pi} \int_{-\infty}^{\infty} \psi_T(\tau) e^{-jw\tau} d\tau \quad (12)$$

$$= \lim_{T \rightarrow \infty} \frac{1}{2\pi T} \int_{-\infty}^{\infty} e^{-jw\tau} d\tau \int_{-\infty}^{\infty} x_T(t)x_T(t + \tau) dt \quad (13)$$

$$= \lim_{T \rightarrow \infty} \frac{1}{2\pi T} \int_{-\infty}^{\infty} dt \int_{-\infty}^{\infty} [x_T(t) e^{jw t}]$$

$$[x_T(t + \tau) e^{-jw(t + \tau)}] d\tau \quad (14)$$

$$= \lim_{T \rightarrow \infty} \frac{1}{2\pi T} \int_{-\infty}^{\infty} x_T(t) e^{j\omega t} dt \int_{-\infty}^{\infty} x_T^*(t_1) e^{-j\omega t_1} dt_1 \quad (15)$$

The two integrals in Equation (15) can be recognized as the Fourier Transform of $x_T(t)$, denoted as $A_T(\omega)$, and the complex conjugate $A_T^*(\omega)$. Equation (15) can then be rewritten as

$$\frac{1}{\pi} \int_{-\infty}^{\infty} \psi(\tau) e^{-j\omega\tau} d\tau = \lim_{T \rightarrow \infty} \frac{A_T(\omega) A_T^*(\omega)}{T} = G(\omega, x) \quad (16)$$

where $G(\omega, x)$ is defined (Lanning and Battin, 1956) as the power density spectrum for a given record of $x(t)$. To obtain the power density spectrum for the ensemble, $G(\omega, x)$ must be averaged over the ensemble as

$$G_{xx}(\omega) = E[G(\omega, x)] = \frac{1}{\pi} \int_{-\infty}^{\infty} E[\psi(\tau)] e^{-j\omega\tau} d\tau \quad (17)$$

where

$$E[\psi(\tau)] = \lim_{T \rightarrow \infty} \frac{1}{2T} \int_{-T}^T E[x(t)x(t+\tau)] dt \quad (18)$$

From Equation (9), our definition of the autocorrelation function, Equation (18) becomes

$$G_{xx}(\omega) = \frac{1}{\pi} \int_{-\infty}^{\infty} e^{-j\omega\tau} d\tau \left[\lim_{T \rightarrow \infty} \frac{1}{2T} \int_{-T}^T \phi_{xx}(t, t+\tau) dt \right] \quad (19)$$

The last equation holds for any random process. If the process $x(t)$ is stationary, the equation is simplified. A stationary process is one in which statistical properties are a function of τ only. Then $\phi_{xx}(t, t+\tau)$ can be rewritten as $\phi_{xx}(\tau)$, and Equation (19) becomes

$$G_{xx}(\omega) = \frac{1}{\pi} \int_{-\infty}^{\infty} \phi_{xx}(\tau) e^{-j\omega\tau} d\tau \quad (20)$$

and

$$\phi_{xx}(\tau) = \int_0^{\infty} G_{xx}(w) \cos w\tau dw \quad (21)$$

Equations (20) and (21) are known as the Wiener-Khinchin relations.

A similar derivation for the cross-correlation and cross-power spectral density for two random processes $x(t)$ and $y(t)$ yields

$$\phi_{xy}(t, t + \tau) = E[x(t)y(t + \tau)] \quad (22)$$

$$G_{xy}(w) = \frac{1}{\pi} \int_{-\infty}^{\infty} e^{-jw\tau} d\tau \left[\lim_{T \rightarrow \infty} \frac{1}{2T} \int_{-T}^T \phi_{xy}(t, t + \tau) dt \right] \quad (23)$$

The principles of autocorrelation and cross-correlation are often used as the basis for radar receiver design. In actual practice, the time limited autocorrelation function is measured as

$$R(\tau, T) = \frac{1}{T} \int_0^T x(t)x(t + \tau) dt \quad (24)$$

That a finite time must be used is the main reason why differences exist between theoretical and experimental results (Bendat, 1956). Figures 1 and 2 show the basic block diagrams for correlation receivers (Skolnik, 1962).

CLUTTER MODELS AND POWER SPECTRUM CALCULATIONS

The analysis of airborne moving target indicator radar effectiveness for detecting targets in the presence of ground clutter requires a knowledge of the clutter signal. Although clutter targets such as buildings, bare hills, or mountains produce echo signals that are constant in both phase and

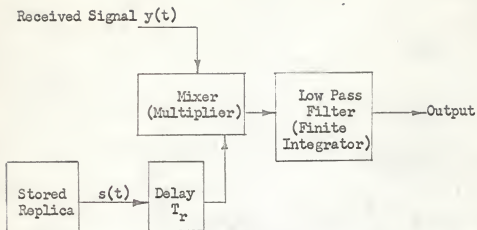


Fig. 1. Block diagram of a cross-correlation receiver.

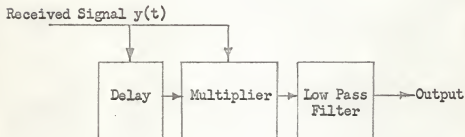


Fig. 2. Block diagram of an autocorrelation receiver.

amplitude as a function of time, there are many types of clutter that cannot be considered as absolutely stationary. Echoes from trees, vegetation, sea, and rain fluctuate with time, and these fluctuations can limit performance of MTI (Skolnik, 1962).

Essentially all analysis of AMTI systems based on random variable theory start with the following reasoning for clutter. The return signal at the radar receiver is assumed to be the vector sum of return signals from a large number of scatterers. These scatterers are assumed to have the same reflectivity, but with each scatterer reflecting with a random phase angle relative to the remaining scatterers. The return signal is usually expressed using the Rice representation for random noise as (Rice, 1948)

$$S(t) = X(t)\cos w_c t - Y(t)\sin w_c t \quad (25)$$

where

$$X(t) = \sum_1^{\infty} a_n \cos(nw - w_c)t + \sum_1^{\infty} b_n \sin(nw - w_c)t \quad (26)$$

$$Y(t) = \sum_1^{\infty} -b_n \cos(nw - w_c)t + \sum_1^{\infty} a_n \sin(nw - w_c)t \quad (27)$$

$X(t)$ and $Y(t)$ are normally distributed random variables with zero mean and standard deviation $\sigma_x = \sigma_y = \sigma$. The signal can be rewritten as

$$S(t) = R(t)\cos(w_c t + \theta_c) \quad (28)$$

and the probability density function for the envelope $R(t)$ can be shown to be (Bendat, 1956) the Rayleigh distribution

$$p(R) = \frac{R}{\sigma^2} \exp(-R^2/2\sigma^2) \quad R \geq 0 \quad (29)$$

If $S(t)$ represents a voltage or current, then the power in the return is

$$W = R^2 \quad (30)$$

and if the average power is $\overline{R^2} = W_0$, then

$$\overline{R^2} = \int_0^{\infty} R^2 p(R) dR = 2\sigma^2 = W_0 \quad (31)$$

Therefore the power probability density function is

$$p(W) = \frac{R}{W_0} \exp(-W/W_0) \quad W \geq 0 \quad (32)$$

A second type of analysis uses what could be termed a deterministic clutter model. These analyses establish an average or a peak clutter power value for a given frequency range. The clutter models vary from strictly deterministic to a combination of random models and deterministic parameters.

Seven papers on AMTI performance analysis illustrating the different techniques were reviewed. Three of the papers by Urkowitz, Bailey, and Remely are examples of theoretical random variable analysis; four papers are grouped under deterministic models; however, the two by Dickey and Welch are a combination approach; and the two by Taylor and Farrell, and Coleman and Hetrich are mainly deterministic.

Random Models

Urkowitz-Clutter Cancellation and Target Enhancement. Urkowitz (1958) assumed a very large number of small scatterers as the basic clutter model. Then using random variable theory he derived the pulse-to-pulse autocorrelation function for an AMTI

system and obtained formulas for MTI cancellation and moving target enhancement.

The residue signal, $R(t)$, can be expressed in terms of the video signal before cancellation, $V(t)$, and the radar repetition period, T , as

$$R(t) = V(t) - V(t + T) \quad (33)$$

The mean square value of the residue can be written as

$$\overline{R^2(t)} = \overline{V^2(t)} - 2\overline{V(t)V(t+T)} + \overline{V^2(t+T)} \quad (34)$$

Assuming that the signal $V(t)$ is stationary, $\overline{V^2(t)} = \overline{V^2(t+T)}$ and that the video autocorrelation function, $\rho(\tau)$ is defined as

$$\rho(\tau) = \frac{\overline{V(t)V(t+\tau)}}{\overline{V^2(t)}} \quad (35)$$

the mean square value $\overline{R^2(t)}$ becomes

$$\overline{R^2(t)} = 2\overline{V^2(t)} [1 - \rho(T)] \quad (36)$$

The cancellation ratio, C_c , is defined in terms of the residue as

$$C_c = \frac{\overline{V_c^2(t)}}{\overline{R_c^2(t)}} = \frac{1}{2[1 - \rho_c(T)]} \quad (37)$$

where the subscript, c , refers to clutter signals. The ratio of moving-target mean square residue to stationary-target mean square residue is defined as enhancement (E), where

$$E = \frac{\overline{R_m^2}}{\overline{R_s^2}} = \frac{1 - \rho_m(T)}{1 - \rho_s(T)} \quad (38)$$

The video autocorrelation function of ground clutter return was then derived. It was assumed that the resolvable ground patch has an azimuthal extent equal to the beamwidth, and a radial

extent approximately equal to $C\tau/2$, where τ is the pulse duration. It was assumed that the illuminated ground patch, in the absence of large reflectors, is made up of a very large number of very small reflectors. These reflectors were assumed to be motionless. The fluctuation in the return is caused by the motion of the aircraft between pulses. The return was assumed to be

$$i_1(t) = \sum_{n=1}^N C_n \cos(\omega_0 t - \phi_n) \quad (39)$$

where

ω_0 = transmitted angular frequency

ϕ_n = random phase angle with uniform distribution $(0, 2\pi)$

Urkowitz used Rice's notation in the following derivations.

Let b^2 equal the uniform reflectivity of the patch where A is the area of the patch, then

$$C_n = \sqrt{\frac{A}{N}} b \quad (40)$$

and

$$i_1(t) = I_1 \cos \omega_0 t + I_2 \sin \omega_0 t \quad (41)$$

$$I_1 = \sqrt{\frac{A}{N}} b \sum_{n=1}^N \cos \phi_n \quad (42)$$

$$I_2 = \sqrt{\frac{A}{N}} b \sum_{n=1}^N \sin \phi_n \quad (43)$$

At a time T later, the second pulse is received and is expressed as

$$i_2(t + T) = \sqrt{\frac{A}{N}} b \sum_{n=1}^N \cos(\omega_0 t + \omega_0 T - \phi_n - \alpha_n) \quad (44)$$

where α_n is not random, but is equal to the phase change between received pulses. Now, $\alpha(r, \theta)$ may be expressed as

$$\alpha(r, \theta) = \frac{4\pi[VrT\cos\theta - (\frac{1}{2})(VT)^2]}{\lambda \sqrt{r^2 + z^2}} \quad (45)$$

where V and V_T are aircraft and target velocities respectively, and

z = altitude

r = ground range to a point in the ground patch

θ = azimuth angle of a point in the ground patch

Equation (44) is then rewritten as

$$i_2(t + T) = I_3 \cos \omega_0(t + T) + I_4 \sin \omega_0(t + T) \quad (46)$$

where

$$I_3 = \sqrt{\frac{A}{N}} B \sum_{n=1}^N \cos(\theta_n + \alpha_n) \quad (47)$$

$$I_4 = \sqrt{\frac{A}{N}} b \sum_{n=1}^N \sin(\theta_n + \alpha_n) \quad (48)$$

The RF mean square clutter current is defined as

$$\overline{i_1^2} = \overline{i_2^2} = \overline{i_3^2} = \overline{i_4^2} = \overline{i_1^2(t)} = \overline{i_2^2(t)} = \mu_0 = \frac{Ab^2}{2} \quad (49)$$

The second-order central moments are defined as

$$\overline{i_1 i_3} = \mu_{13} = \frac{\mu_0}{A} \iint \cos \alpha(r, \theta) r dr d\theta \quad (50)$$

$$\overline{i_1 i_4} = \mu_{14} = \frac{\mu_0}{A} \iint \sin \alpha(r, \theta) r dr d\theta \quad (51)$$

In order to simplify notation, the parameter β was defined as

$$\beta^2 = \frac{\mu_{13}^2 + \mu_{14}^2}{\mu_0^2} \quad (52)$$

The above statistical averages were derived by George (1952) but

Urkowitz rewrites them in Rice's notation. The integrals (50) and (51) are known as the radar "scatter integrals". (Computations Lab, 1952). In the absence of a target, the square-law video autocorrelation function is

$$\rho_c(\tau) = \frac{1 + \beta^2}{2} \quad (53)$$

Next, Urkowitz considered the case of a single-point object plus the ground clutter. It was assumed that the radar return from the object is of constant amplitude and frequency. The first return is then

$$i_1(t) = P \cos w_0 t + I_1 \cos w_0 t + I_2 \sin w_0 t \quad (54)$$

where P is the amplitude of the object return. The second return is given as

$$i_2(t + \tau) = P \cos(w_0 t + w_0 \tau - \gamma) + I_3 \cos w_0(t + \tau) + I_4 \sin w_0(t + \tau) \quad (55)$$

where γ is the phase change of the return from the object and is derived from

$$\gamma = \frac{4\pi}{\lambda} (S_1 - S_2) \quad (56)$$

where

$$S_1 = \sqrt{r_a^2 + z^2} \quad (57)$$

$$S_2 = \left[(r_a \cos \theta_a + v_T r \cos \eta - v)^2 + (r_a \sin \theta_a + v_T r \sin \eta)^2 \right]^{1/2} \quad (58)$$

Urkowitz's complete autocorrelation function after a square-law device is

$$\bar{\Psi}(\tau) = (P^2/2 + \mu_0)^2 + \frac{P^4 \cos^2(w_0\tau - \gamma)}{8} + 2P^2\psi(\tau) \cos(w_0\tau - \gamma) + 2\psi^2(\tau) \quad (59)$$

where, $\psi(\tau)$ is the RF autocorrelation function of the ground clutter return given by

$$\psi(\tau) = \frac{i_1(t) i_2(t+\tau)}{i_1(t) i_2(t+\tau)} = \left[\frac{1}{2} \frac{A}{N} b^2 \sum_{n=1}^N \cos \alpha_n \right] \cos w_0\tau + \left[\frac{1}{2} \frac{A}{N} b^2 \sum_{n=1}^N \sin \alpha_n \right] \sin w_0\tau \quad (60)$$

For large N , the summation becomes an integral and Equation (60) becomes

$$\psi(\tau) = \mu_{13} \cos w_0\tau + \mu_{14} \sin w_0\tau \quad (61)$$

The normalized video autocorrelation function is

$$\bar{\Phi}_T(\tau) = \frac{(x+1)^2 + 2x \cos(\theta_0 - \gamma) + \beta^2}{(x+1)^2 + 2x + 1} \quad (62)$$

where

$$x = P^2/2\mu_0 = \text{RF signal-to-clutter power ratio}$$

$$\theta_0 = \arctan(\mu_{14}/\mu_{13}).$$

These results are now combined in final expressions for clutter cancellation and moving target enhancement. When Equation (53) is substituted into Equation (37), the clutter cancellation ratio becomes

$$C_c = \frac{1}{1 - \beta^2} \quad (63)$$

The subscripts s and m are used to distinguish the autocorrelation functions for stationary and moving targets. For a moving target the function is

$$\phi_m(T) = \frac{(x+1)^2 + 2x\cos(\theta_o - \gamma_m) + \beta^2}{(x+1)^2 + 2x + 1} \quad (64)$$

whereas, for a stationary target, it is

$$\phi_s(T) = \frac{(x+1)^2 + 2x\cos(\theta_o - \gamma_s) + \beta^2}{(x+1)^2 + 2x + 1} \quad (65)$$

When Equations (65) and (66) are substituted into Equation (38), the result for moving target enhancement is

$$E = \frac{2x[1 - \cos(\theta_o - \gamma_m)] + 1/C_c}{2x[1 - \cos(\theta_o - \gamma_s)] + 1/C_c} \quad (66)$$

Bailey-Clutter Cancellation. Bailey (1963) calculated the probability of detection for a coherent AMTI radar described by the block diagram of Fig. 3.

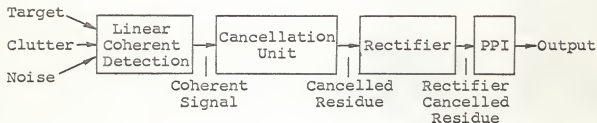


Fig. 3. Coherent AMTI block diagram

The signal is coherently detected and enters the cancellation unit where it is delayed τ seconds by a delay line. This signal is subtracted from a signal occurring τ seconds later. The so-called "cancelled residues" are then rectified and displayed on a plan position indicator to show the location of the target.

The probability of detecting a target traveling at a velocity during any one scan is

$$P_D = \int_{Z_{0B}}^{\infty} P_1(Z_0) dZ_0 \quad (67)$$

where

$P_1(Z_0)$ = probability density function of target and clutter
at output

Z_{0B} = threshold level.

The probability of false alarm is

$$P_f = \int_{Z_{0B}}^{\infty} P_0(Z_0) dZ_0 \quad (68)$$

where

$P_0(Z_0)$ = probability density of clutter alone.

In order to determine $P_1(Z_0)$ and $P_0(Z_0)$, it is necessary to determine the following probability density functions:

1. The joint density function at the output of the receiver,

$$P[R(t), \theta(t); R(t - \tau), \theta(t - \tau)] \quad (69)$$

2. The second probability density function at the output of the phase cancellation unit.

$$P[\theta(t) - \theta(t - \tau)] \quad (70)$$

3. The second probability density function at the output of the rectifier.

$$P[\theta(t) - \theta(t - \tau)] \quad (71)$$

Bailey assumed a Rayleigh ground and expressed the input signal

as

$$C_q(t) = \sum_{K=0}^N \sqrt{\sigma_K} \cos(\omega_0 t + \phi_K - \psi_K) \quad (72)$$

where

$C_q(t)$ = current from the q th pulse

w_0 = carrier frequency

β_k = phase of the kth scatterer

$q\psi_k$ = change in phase angle between the first and qth look

σ_k = power received from kth scatterer.

This equation is expanded and rewritten as

$$C_q(t) = X_q \cos w_0 t + Y_q \sin w_0 t \quad (73)$$

$$X_q = \sum_{k=0}^N \sqrt{\sigma_k} \cos(\beta_k - q\psi_k) \quad (74)$$

$$Y_q = \sum_{k=0}^N \sqrt{\sigma_k} \sin(\beta_k - q\psi_k) \quad (75)$$

The target signal was written as

$$S(t) = \sqrt{2S} f(t) \cos(w_T t + \alpha) \cos w_0 t \quad (76)$$

where

w_T = 2π times center frequency of the signal power density spectrum

α = random phase angle which is constant for any particular target

S = RMS signal power

$f(t)$ = term that accounts for target fluctuations.

The probability density function was then calculated as

$$P\{[S(t) + C(t)], [S(t - \tau) + C(t - \tau)]\} = P\{R(t), \theta(t); R(t - \tau), \theta(t - \tau)\} \quad (77)$$

where

$$S(t) + C(t) = [X(t) + A(t)] \cos w_0 t + Y(t) \sin w_0 t \quad (78)$$

The final result requires determination of a four-dimensional probability distribution. The final expression for the joint

probability density function for the amplitude of a target-plus-clutter signal arriving at $(t - \tau)$ and one arriving at (t) , with a linearly detecting receiver, was given as

$$P(R_1, R_2, \theta_1, \theta_2) = \frac{R_1 R_2}{4\pi^2 A} \exp\left\{-\frac{1}{2A} \left[\sigma^2 (R_1^2 + R_2^2) - 2\mu_{12} R_1 R_2 \cos(\theta_1 - \theta_2) - 2\mu_{14} R_1 R_2 \sin(\theta_1 - \theta_2) \right]\right\} \quad (79)$$

where

$$R_1 = \sqrt{[x(t) + A(t)]^2 + [y(t)]^2}$$

$$\theta_1 = \arctan\left\{\frac{y(t)}{x(t) + A(t)}\right\}$$

$$R_2 = \sqrt{[x(t - \tau) + A(t - \tau)]^2 + [y(t - \tau)]^2}$$

$$\theta_2 = \arctan\left\{\frac{y(t - \tau)}{x(t - \tau) + A(t - \tau)}\right\}$$

In terms of the power density spectrums of the target signal and the clutter.

$$A' = \sigma^4 - \mu_{12}^2 - \mu_{14}^2$$

$$\sigma^2 = \int_0^{\infty} [G_T(f - f_T) + G_C(f - f_C)] df$$

$$\mu_{12} = \int_0^{\infty} [G_T(f - f_T) + G_C(f - f_C)] \cos 2\pi(f - f_C) df$$

$$\mu_{14} = \int_0^{\infty} [G_T(f - f_T) + G_C(f - f_C)] \sin 2\pi(f - f_C) df$$

Next the second probability density function $P(|\varnothing|)$ at the output of the phase cancellation unit was derived. The phase difference was defined as

$$\varnothing = \theta_1 - \theta_2 \quad (80)$$

and the probability density function of the output is

$$P(|\phi|) = P(\phi) + P(-\phi) \quad (81)$$

After a change of variable and integrating out R_1 and R_2 the density function is

$$P(\phi) = \frac{A'}{2\pi\sigma^4} \left[\frac{(1 - \beta^2)^{1/2} + \beta(\pi - \arccos \beta)}{(1 - \beta^2)^{3/2}} \right] \quad (82)$$

where

$$\beta = \frac{\mu_{12}}{\sigma^2} \cos\phi + \frac{\mu_{14}}{\sigma^2} \sin\phi$$

The final expression for $P(|\phi|)$ was then obtained by evaluating σ^2 , μ_{12} , and μ_{14} . The power density spectrum of both the clutter and target was assumed to be gaussian as given by

$$G_T(f - f_T) = \frac{S}{\sqrt{2\pi}\sigma_s} \exp\left\{- (f - f_T)^2 / 2\sigma_s^2\right\} \quad (83)$$

and

$$G_C(f - f_C) = \frac{\psi_0}{\sqrt{2\pi}\sigma_c} \exp\left\{- (f - f_C)^2 / 2\sigma_c^2\right\} \quad (84)$$

After integrating and making some simplifying approximations Bailey obtained

$$\mu_{12} = \psi_0 \exp(-2\pi^2 \sigma_c^2 \tau^2) + S \cos 2\pi f_D \tau \quad (85)$$

$$\mu_{14} = S \sin 2\pi f_D \tau \quad (86)$$

$$\sigma^2 = \psi_0 + S \quad (87)$$

Equations (85) - (87) are then substituted into Equations (81) and (82) to obtain the final expression for $P(|\phi|) = P(Z_p)$.

The preceding results are then combined in the form of a clutter cancellation ratio, C_c . On a phase basis, the clutter cancellation ratio is

$$C_c = 10 \log \left\{ \frac{\int_0^\pi (z_p)^2 P(z_p) dz_p \text{ (correlated)}}{\int_0^\pi (z_p)^2 P(z_p) dz_p \text{ (uncorrelated)}} \right\} \quad (88)$$

Bailey also gave a numerical evaluation of the probability of detection (P_D), and the probability of false alarm (P_F). These results are expressed in graphical form and are not reproduced here. The assumption for clutter and the method of analysis are of primary interest to this work.

Remley - Linear Signal Delay. Remley (1963) was concerned with the output of a cross-correlator detector under the conditions of a constant delay rate. The output signal of a one-dimensional cross-correlator was calculated for a general signal spectrum under the assumption of a constant delay rate, but otherwise ideal conditions. The analysis was directed primarily at the problem of coherent passive detection, but the results are directly applicable to any ideal, one-dimensional, coherent detector where the signal delay may be approximated by a linear function of time. For example, a coherent echo ranging system where a noiselike waveform is stored for correlation with the return energy.

The two inputs to a cross correlator are denoted as the signals and additive noise given as

$$v_1(t) = S_1(t) + n_1(t) \quad (89)$$

$$v_2(t) = S_2(t) + n_2(t) \quad (90)$$

It was assumed that there is no correlation between $n_1(t)$ and

$n_2(t)$ or between signal and noise. Each component was assumed to be stationary with zero mean and signal powers were assumed equal. The instantaneous delay of the signals, Δt , was defined as

$$S_1(t) = S_2[t - \Delta t] \quad (91)$$

Over a short interval $\Delta(t)$ was assumed to be a linear function of time, or

$$\Delta t = \tau_0 + \dot{\tau}(t - t_0); \quad |t - t_0| \leq \frac{1}{2}(T + \tau_{\max}) \quad (92)$$

where

$$\tau_0 = \text{delay at } t = t_0$$

$$\dot{\tau} = \text{delay rate}$$

T = integration time of the correlator

τ_{\max} = parametric time interval for which the correlation is to be computed.

Then Equations (91) and (92) yield

$$S_1(t) = S_2[t - \dot{\tau}(t - t_0) - \tau_0] \quad (93)$$

The correlator output at $(t = t_0)$ was defined as

$$R(\tau) = \frac{1}{T} \int_{(t_0 - \frac{1}{2}T)}^{(t_0 + \frac{1}{2}T)} v_2(t) v_1(t + \tau) dt \quad (94)$$

Because of the finite integration time, the correlator output $R(\tau)$ is a random variate. Therefore the output signal was defined as the expectation of $R(\tau)$,

$$E[R^j(\tau)] = \frac{1}{T} \int_{(t_0 - \frac{1}{2}T)}^{(t_0 + \frac{1}{2}T)} E[v_2^j(t) v_1^j(t + \tau)] dt \quad (95)$$

where $R^j(\tau)$ is the j^{th} member of the ensemble. After substitution of Equations (90) and (93) into (95) and evaluation of the integral

the result was

$$E[R^j(\tau)] = \sigma_s^2 h(\tau) * \rho_1[\tau - \tau_0/(1 - \dot{\tau})] \quad (96)$$

where

$$\rho_1(\tau) = \rho_2[\tau(1 - \dot{\tau})] = \text{autocorrelation functions of } S_1(t) \\ \text{and } S_2(t)$$

$$h(t) = \begin{cases} (1 - \dot{\tau})/2T; & \text{if } |t| \leq \dot{\tau}T/2(1 - \dot{\tau}) \\ 0 & \text{elsewhere} \end{cases}$$

* = convolution

Equation (96) was then evaluated by use of the convolution theorem, which yielded

$$F[h(\tau)] = \frac{\sin[\pi f \dot{\tau} T/(1 - \dot{\tau})]}{[\pi f \dot{\tau} T/(1 - \dot{\tau})]} \quad (97)$$

and

$$F\{\rho_1[\tau - \tau_0/(1 - \dot{\tau})]\} = P_1(f) \exp[-2\pi j f \tau_0/(1 - \dot{\tau})] \quad (98)$$

where $P_1(f)$ is the Fourier transform of $\rho_1(\tau)$ and is called the normalized power spectrum of $S_1(t)$.

Combining equations (96), (97), and (98), the cross spectrum of the expected correlator output was calculated to be

$$F\{E[R^j(\tau)]\} = \sigma_s^2 P_1(f) \exp[-2\pi j f \tau_0/(1 - \dot{\tau})] \\ \times \frac{\sin[\pi f \dot{\tau} T/(1 - \dot{\tau})]}{[\pi f \dot{\tau} T/(1 - \dot{\tau})]} \quad (99)$$

Inspection of equation (99) shows that the effect of the delay rate is equivalent to passing the ideal correlator output ($\dot{\tau} = 0$) through a low-pass filter whose transfer function is

$$T(f) = \exp[-2\pi j f \tau_0/(1 - \dot{\tau})] \\ \times \frac{\sin[\pi f \dot{\tau} T/(1 - \dot{\tau})]}{[\pi f \dot{\tau} T/(1 - \dot{\tau})]} \quad (100)$$

Remley then derived an expression for peak output signal-to-

noise ratio for an active detector system. One input to the system was assumed to be a known signal and the second input was assumed to be noise. The noise output is given as

$$N_o = \sigma_s^2 \sigma_n^2 / (2W_n T) \quad (101)$$

where

W_n = equivalent rectangular bandwidth of the noise.

The final expression for signal to noise ratio was given as

$$(S/N)_o = 2W_n T \left\{ (S/N)_i \frac{2(1-\tau)}{\tau T} \int_0^{\tau T/2(1-\tau)} \rho_1(t) dt \right\}^2 \quad (102)$$

Finally it was shown that for zero delay rate $(S/N)_o$ is a linearly increasing function of the time-bandwidth product, but for non-zero delay rates, maximum points exist, when the signal is white noise.

Deterministic Models

Dickey - Clutter Cancellation. Dickey's paper (1953) considered the effect of antenna motion on clutter cancellation. A stationary target and a perfectly stable radar platform were assumed. The clutter cancellation as a function of antenna pointing angle in azimuth was calculated. The mean square value of the residual clutter was found to be the sum of four components, one due to antenna rotation and three others due to aircraft motion. The quantity ϵ was defined as

$$\epsilon = \frac{\text{Mean Square Pulse-to Pulse Voltage Change}}{\text{Mean Square Voltage}} \quad (103)$$

The received signal was assumed to result from a large number of small component signals with random phase. The amplitudes of the individual components of the signal are weighted as a

function of the azimuth antenna pattern and as a function of the elevation angle. In the case of a short duration pulse, the elevation function depends on the pulse width and shape. The variations in signal strength, which prevent complete cancellation, are said to be caused by changes in relative phase of various components due to displacement of the radar platform and change in the amplitude of various components due to rotation of the antenna, during the interpulse period. Although the component phase angles are random, the changes in relative phase of a component during the interpulse period can be calculated.

The displacement of the antenna during the interpulse period is expressed in terms of its components along X, Y, Z axes of an orthogonal coordinate system. The Z axis is oriented along the antenna boresight. The displacement is then

$$X = VT \sin(\theta - \theta_0) \quad (104)$$

$$Y = VT \cos(\theta - \theta_0) \sin \phi \quad (105)$$

$$Z = VT \cos(\theta - \theta_0) \cos \phi \quad (106)$$

where

V = velocity of the aircraft

T = time interval between pulses

θ, ϕ = azimuth and elevation angles respectively, measured from Z

θ_0, ϕ_0 = azimuth and elevation angles of the direction of motion. The function $F(\theta, \phi)$, which expresses the phase shift produced by a given antenna displacement, is given as

$$F(\theta, \phi) = \frac{4\pi}{\lambda} (X \sin \theta + Y \cos \theta \sin \phi + Z (\cos \theta \cos \phi)) \quad (107)$$

or assuming a small beamwidth, Equation (107) becomes

$$F(\theta, \phi) = \frac{4\pi}{\lambda} (X\theta + Y\phi - Z(\theta^2 + \phi^2)) \quad (108)$$

The weighting functions $A(\theta)$ and $B(\phi)$ are then defined as

$A(\theta)$ = round-trip voltage antenna pattern in azimuth

$B(\phi)$ = elevation weighting function.

The vector difference between two successive signals is then found to be

$$\begin{aligned} D = & A(\theta + \frac{1}{2}w_a T)B(\phi) \exp(j\frac{1}{2}F(\theta, \phi)) \\ & - A(\theta - \frac{1}{2}w_a T)B(\phi) \exp(-j\frac{1}{2}F(\theta, \phi)) \end{aligned} \quad (109)$$

where

w_a = angular rotation rate of the antenna.

Combining Equations (103) and (109), the quantity ϵ becomes

$$\epsilon = \frac{\int_{-\infty}^{+\infty} \int |D|^2 d\theta d\phi}{\int_{-\infty}^{+\infty} \int |A(\theta)B(\phi)|^2 d\theta d\phi} \quad (110)$$

Equations (108) and (110) were then combined and the results reduced to the form

$$\epsilon = \epsilon_R + \epsilon_X + \epsilon_Y + \epsilon_Z \quad (111)$$

where ϵ_R is the residual clutter component due to antenna rotation, and ϵ_X , ϵ_Y , ϵ_Z are the residual clutter components due to radar displacement along the X, Y, Z axes. These components were then calculated using rectangular, gaussian, and $(\sin x)/x$ round-trip azimuth antenna patterns. From these results, the clutter attenuation for a given set of parameters was calculated. These results show that the greatest clutter attenuation or cancellation occurs within 15° to 20° of the aircraft direction

of motion, whereas the least attenuation occurs at 90° to the motion. For the parameters selected there was a difference of 24 db between the maximum and the minimum cancellation.

Coleman and Hetrich - Ground Clutter. Coleman and Hetrich (1961) presented a method for the calculation of approximate ground clutter power return based on an approximation to the return from a given doppler frequency region. Figure 4 shows the basic clutter geometry used in the derivation. The intersection of the cone with the ground is a hyperbola for horizontal flight, and it represents the locus of all points on the ground having the given relative velocities with respect to the radar. The hyperbola also represents the locus of all points on the ground which reflect clutter having the same doppler frequency shift, f_d , where

$$f_d = 2v/\lambda \quad (112)$$

The radar clutter spectrum may be subdivided into a finite number of equal contiguous doppler increments, Δf_d , between $f_o - f_v$ and $f_o + f_v$, where f_o is the carrier frequency and f_v is the maximum doppler frequency shift.

Size and range of the clutter reflecting area is determined by the relationships in Fig. 5. The increment Δd_n is the distance between the n^{th} hyperbola and the $n + 1$ hyperbola and is given by

$$\Delta d_n = \frac{(n - 1)H\Delta f_d \lambda}{\sqrt{(103V)^2 - (n - 1)^2(\Delta f_d \lambda)^2}} \quad (113)$$

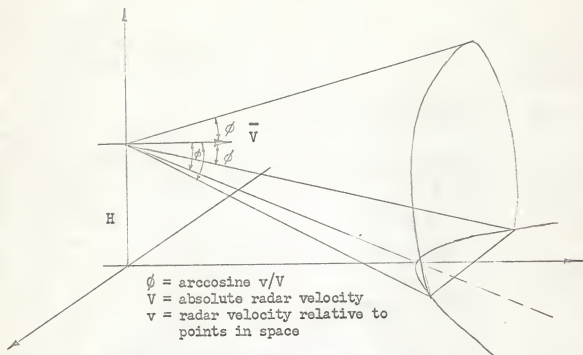


Fig. 4. Constant doppler loci.

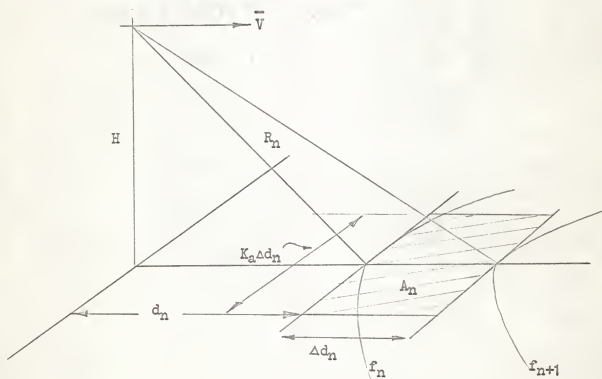


Fig. 5. Clutter reflecting area.

where

Δf_d = doppler increment in cps

$$n = 1, 2, 3, \dots, \left(1 + \frac{103V}{f_d}\right) = 1 + f_d/\Delta f_d$$

H = altitude in the same units as d_n

λ = wavelength in centimeters

V = velocity in knots

The effective scattering area, which represents the n^{th} doppler region, is assumed to be a rectangle, one side of which is Δd_n long and the other side is $Ka\Delta d_n$. The incremental area, A_n , is given by

$$A_n = Ka(\Delta d_n)^2 \quad (114)$$

The constant, Ka , was chosen as unity because of the R^{-4} relationship causing most of the power in the return to come from the area nearest the radar. The slant range, R_n , to the area A_n is given by

$$R_n = \sqrt{H^2 + d_n^2} \quad (115)$$

The clutter power return from the n^{th} area was then derived from the basic radar equation as

$$P_{cn} = \frac{P_1 G_n^2 \lambda^2 \sigma_{oA_n}}{(4\pi)^3 R_n^4} \quad (116)$$

where

P_{cn} = clutter power from A_n

P_1 = transmitted power in first PRF spectral line

For a pulse doppler radar using narrow band detection filters, the power of interest is that contained in the center spectral line. When a pulse doppler radar transmits peak power,

P_t , at a duty cycle, d , the power in the carrier or center spectral line, P_{csl} , is

$$P_{csl} = P_t d^2 \quad (117)$$

where

d = pulse width times the pulse repetition frequency (τf_r).

The power in the spectral line which is $m f_r$ cycles per second from the carrier has an amplitude

$$P_m = P_t d^2 \left[\frac{\sin m\pi d}{m\pi d} \right]^2 \quad (118)$$

and

$$P_1 = P_t d^2 \left[\frac{\sin \pi d}{\pi d} \right]^2 \quad \text{for } m = 1 \quad (119)$$

The gain was determined from the geometry of the problem and the antenna pattern. The reflection coefficient, σ_o was determined by the type of terrain. Finally, the clutter power density was expressed as

$$G_{cn}(\Delta f_d) = P_{cn} / \Delta f_d \quad (120)$$

The major approximation made in this development is that return from areas between the isodops, but outside the defined ground patch, is negligible.

Welch - Radar Terrain Return Fading Spectra. In work performed by the Physical Science Laboratory of New Mexico State University for Sandia Corporation, (Welch, 1960) a method similar to Hetrich's was used to compute the clutter power from incremental ground areas. However, the New Mexico procedure calculated the return from all areas defined by a grid related to flight conditions, instead of approximating A_n . The basic approach is the same for

calculation of power return. This power spectrum is then used to calculate a pulse-to-pulse variance spectrum, $V(f)$,

$$V(f) = 2 \int_{-\infty}^{+\infty} P(g)P(g - f)dg \quad (121)$$

where

$P(f)$ = calculated power spectrum.

The ground plane was divided into a set of incremental areas by means of two families of curves, namely,

1. A set of concentric circles (loci of constant angle of incidence) centered about the point directly beneath the radar.
2. A set of hyperbolas, with the radar at the foci, as a function of the angle between the radar velocity vector and the ground point.

A grid was constructed for the horizontal case and the areas were measured by a planimeter, weighted by $\cos^4\theta$ and tabulated. The RF power spectrum was computed by the basic radar equation applied to the incremental areas and the results were summed over a given doppler frequency band. The calculations were restricted to angles of incidence near the vertical. Chia (1960) in his master's thesis at the University of New Mexico developed a computer program for the above model. This work and the paper by Farrell and Taylor form the basis for the model developed in this paper.

Farrell and Taylor - Doppler Radar Clutter. J. L. Farrell and R. L. Taylor (1963) have extended the method of Coleman and

Hetrich (1961) and derived a method for computation of the clutter spectrum for doppler radar. They were interested in obtaining a relatively simple and accurate method of calculating the clutter spectrum for both main beam and side-lobe contributions.

The following system restrictions were used throughout their analysis.

1. The antenna beamwidth $\leq 15^\circ$.
2. Antenna E-plane and H-plane beamwidths are equal.
3. The transmitter duty ratio is the reciprocal of an integral number, so that the receiver is divided into an integral number of range gates. During each interpulse period, each gate is opened only once, for a time interval equal to the duration of the transmitted pulse.
4. The radar detection range is far in excess of the maximum unambiguous radar range.
5. The clutter return is from a large number of scatterers, each of which reflects the same percentage of energy when illuminated at normal incidence.

The basic approach was to divide the spectrum into three regions, which correspond to the antenna main beam, the first side-lobe, and the remaining lobes. Side-lobe clutter is taken to be stationary or, the clutter is assumed to be uniformly distributed in all range gates. The main beam clutter is in general time-varying. Upper and lower bounds are determined by computing the spectrum under the conditions, all main beam clutter is in a

single range gate, and that it is uniformly distributed among all range gates.

In the derivation of the side-lobe clutter formulas, it was assumed that the antenna gain was constant within the n^{th} isodop. (See Fig. 6.) The total clutter, C_n , returned from beyond the n^{th} isodop was determined from

$$C_n = \int_{\theta_1}^{\theta_2} \int_{\phi_1}^{\phi_2} \frac{\bar{P}G^2\lambda^2\delta\sigma_0}{(4\pi)^3h^2} \sin\theta \cos\theta \, d\theta \, d\phi \quad (122)$$

After considerable manipulation and substitution, C_n was found to be

$$C_n = \frac{\bar{P}G^2\lambda^2\delta\sigma_0}{(4\pi)^3h^2} (\gamma_n) \quad (123)$$

where

$$\gamma_n = \frac{\pi}{2} - \arcsin\left(\frac{\cos \gamma_n}{\cos \varphi}\right) - \cos \gamma_n \sqrt{\cos^2 \varphi - \cos^2 \gamma_n} + \left[\frac{\pi}{2} + \arcsin\left(\frac{\tan \varphi}{\tan \gamma_n}\right)\right] \sin \varphi \sin^2 \gamma_n \quad (124)$$

An approximation was introduced for $\varphi < 45^\circ$, in order to simplify the final expression to

$$\gamma_n - \gamma_{(n+1)} \approx \gamma_1 - \gamma_2 \quad (125)$$

and

$$\gamma_1 - \gamma_2 \approx \frac{\lambda B}{V} \cos \varphi \quad (126)$$

This result was then used in deriving b_n as Equation (138).

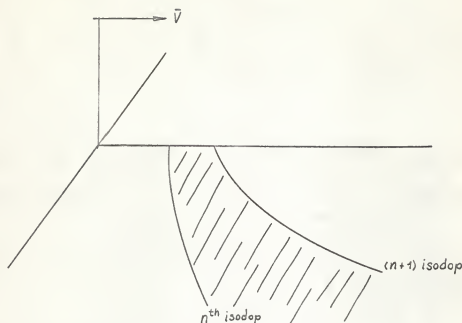


Fig. 6. Area of n^{th} isodop.

Derivation of the main beam clutter formulas was based on a symmetrical antenna pattern. Constant gain cones within the antenna main beam intersect the ground in elliptical figures. Then for the area between two ellipses separated by a small angle, the gain was assumed to be constant. The return from this area was obtained by integrating the expression

$$dC_m(\alpha) = 2K_1 \alpha \exp\left\{-8[\ln 2] \left(\frac{\alpha}{\alpha_1}\right)^2\right\} d\alpha \quad (127)$$

over the ellipse defined by the conic generating angle (α_1), between the limits ($\alpha = 0$) and ($\alpha = \alpha_1$). Again after much manipulation and substitution the final result given in Equation (134) was obtained.

The following is a summary of the procedures for calculation of clutter-to-thermal noise ratio for any given geometric relationship as given by Farrell and Taylor (1963). The following

parameters are the required inputs for the calculations.

<u>Symbol</u>	<u>Nomenclature</u>	<u>Units</u>
d	Transmitter duty ratio	-----
F	Receiver noise figure	-----
G	Peak one-way power gain of antenna	-----
g	Normalized one-way power gain of first side lobe (See Fig. 7)	-----
h	Interceptor altitude	Feet
P	Peak transmitted power	Watts
V_c	Target closing rate	fps
V	Interceptor speed	fps
δ	Radar loss factor	-----
ζ	Interceptor dive angle (+ downward)	Radians
θ	One-way half power beamwidth of antenna	Radians
Λ	Angle between antenna axis and interceptor velocity vector ($0 \leq \Lambda \leq \pi$)	Radians
λ	r-f wavelength	Centi-meters
μ_1	Edge of antenna main beam	} See Fig. 7 Radians
μ_2	Edge of first side lobe	
ξ	Antenna angle off horizontal (positive downward)	Radians

The clutter computation is performed as follows:

1. If the ratio (V_c/V) is greater than unity, the target is in the clutter-free region. If the ratio is less than unity, proceed below.
2. If ($\xi + \mu_1$) is negative, proceed to step 3. If positive,

test whether the target is in main beam clutter (MBC) by the inequality

$$V \cos (\Delta + \mu_1) \leq V_c \leq V \cos (\Delta - \mu_1) \quad (128)$$

3. If the target is not in main beam clutter, check the first side lobe criterion by the inequality:

$$V \cos (\Delta + \mu_2) \leq V_c \leq V \cos (\Delta - \mu_2) \quad (129)$$

If this holds, set the normalized antenna gain (g) at g_1 . If neither of the inequalities (128), (129) hold, compute the mean one-way side lobe power gain (g_2) by:

$$g = 1/G_0 - \epsilon^2/16 [\ln 2] \quad (130)$$

(Do not use approximate gain-beamwidth relations with this formula; g_2 is the difference of two numbers close together.) Set (g) equal to g_2 .

4. Compute the doppler angle (γ_n) and the incidence angle (i) by:

$$\gamma_n = \text{Arccos} (V_c/V) \quad (131)$$

$$i = 90 - (\gamma_n + \xi) \quad (132)$$

Determine the reflection coefficient (σ_0) from the incidence angle and the wavelength.

5. If the target is in main beam clutter, compute the center doppler frequency (f_0) by:

$$f_0 = \frac{61V}{\lambda} \cos \Delta \text{ cps} \quad (133)$$

Where f_0 is the doppler frequency at the center of the MBC spectrum. Compute the maximum and minimum peak power spectra by equations (134) - (137).

$$W_{\max}(f_0) = \frac{10^{-8} P_d G_o^2 \lambda^3 \sigma_o \delta \sin \xi}{h^2 v \sin \Delta} \text{ watts/cps} \quad (134)$$

which is the maximum peak power at f_0 .

$$W_{\max}(f_0 \pm \Delta f) = W_{\max}(f_0) \operatorname{erfc} \left\{ \frac{0.0387 \lambda \Delta f}{v \sin \Delta} \right\} \text{ watts/cps} \quad (135)$$

which is the overall shape of the spectrum.

$$W_{\min}(f_0 \pm \Delta f) = dW_{\max}(f_0 \pm \Delta f) \text{ watts/cps} \quad (136)$$

which is the minimum peak power spectrum.

The actual peak power density spectrum will lie between these boundaries. Compute the clutter-to-thermal noise ratio (β) by

$$\beta(f_0 \pm \Delta f) = \frac{W(f_0 \pm \Delta f)}{\eta F} \quad (137)$$

where

$$\eta = 298^\circ \text{K} \times \text{Boltzman's Constant (Power spectral density of thermal noise)} = 4.12 \times 10^{-21} \text{ watts/cps}$$

Note that both main beam and first sidelobe clutter are present in the "main beam clutter region". Compute both and use the larger value for clutter level estimation.

6. If the target is in side lobe clutter, compute the clutter-to-thermal noise ratio (b_n) by

$$b_n = 4.3 \times 10^{12} \frac{P_d^2 G_o^2 g^2 \lambda^3 \sigma_o \delta}{F h^2 v} \cos \xi \quad (138)$$

The antenna pattern was divided into three regions as shown in Fig. 7. In the main lobe region, the normalized one-way power gain was approximated by the gaussian function

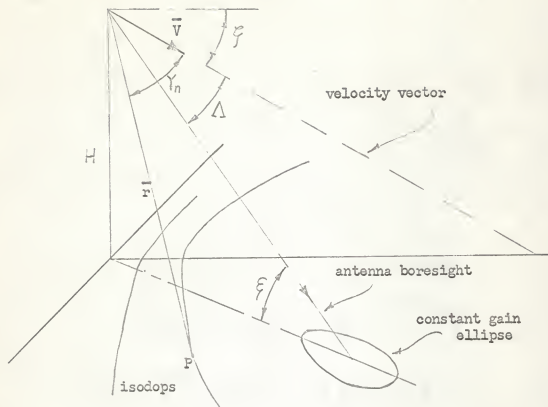


Fig. 7. Clutter geometry.

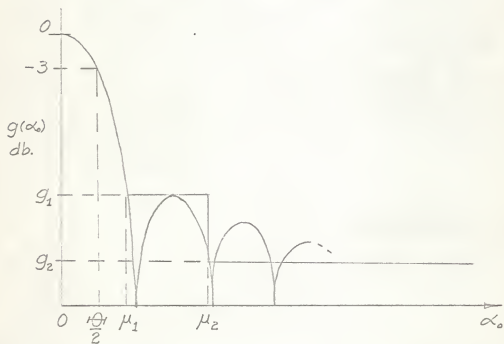


Fig. 8. Normalized antenna gain vs. angle off boresight

$$g(\alpha) = \exp\left[(-4)\left(\frac{\alpha}{\mu_1}\right)^2 \ln 2\right] \quad 0 \leq \alpha \leq \mu_1 \quad (139)$$

and normalized side lobe gain is

$$g = g_1 \quad \mu_1 < \alpha \leq \mu_2 \quad (140)$$

$$g = g_2 \quad \alpha > \mu_2 \quad (141)$$

The peak of the first side lobe was taken from the antenna pattern as shown in Fig. 7. Beyond the first sidelobe, the mean sidelobe gain was calculated using Equation (130).

In Section 5 of this report, the clutter geometry and notation of Farrell and Taylor is used to formulate a mathematical model for the calculation of ground clutter power spectrum.

MATHEMATICAL MODEL FOR GROUND CLUTTER POWER SPECTRUM FOR AN AIRBORNE PULSE RADAR

Clutter Geometry

Relative motion between the radar platform and a point on the ground produces a doppler frequency shift in the return signal. This frequency shift is directly proportional to the closing rate (or range rate) between the radar and the point on the ground. In general the velocity vector of the radar may be oriented at any angle with respect to the ground plane, however, the two cases of interest are when the radar is in horizontal flight or approaching the ground plane in a dive angle. When the radar is in a climb, clutter is not usually a problem. The basic relationships for the clutter model are derived from the geometry of Fig. 9.

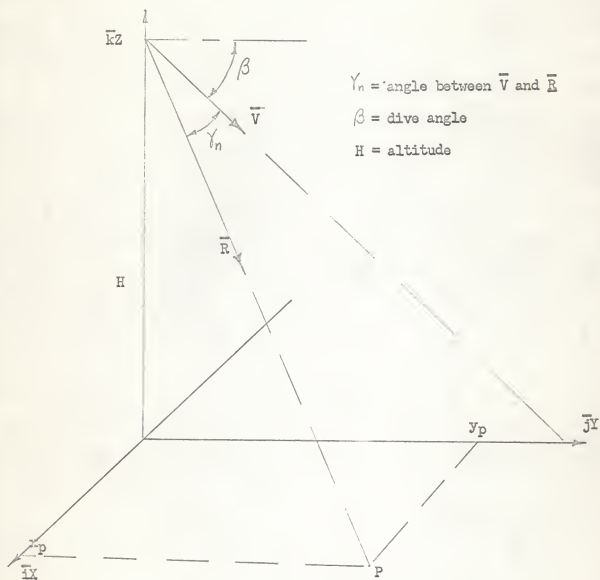


Fig. 9. Clutter geometry.

In Fig. 9, the x-y plane is the ground plane, \bar{V} is the velocity vector in the y-z plane, and \bar{R} is the range vector to point P. (Farrell and Taylor, 1963) The coordinate system is defined by the unit vectors \bar{i}_x , \bar{j}_y , \bar{k}_z , with positive sense as shown in Fig. 9. The vectors \bar{V} and \bar{R} can be written as

$$\bar{V} = \bar{j}_y V \cos \beta - \bar{k}_z V \sin \beta \quad (142)$$

$$\bar{R} = \bar{i}_x R + \bar{j}_y y - \bar{k}_z z \quad (143)$$

The range rate between point P and the radar is the dot product

$$\frac{1}{R} (\bar{R} \cdot \bar{V}) = V \cos \gamma_n = \frac{1}{R} (V_y \cos \beta + V_H \sin \beta) \quad (144)$$

All points on the ground having equal range rate must lie on a loci (isodop) generated by a range vector which has a constant angle (γ_n) with the velocity vector. Solving for $\cos \gamma_n$, one obtains (Farrell and Taylor, 1963)

$$\frac{(\bar{R} \cdot \bar{V})}{RV} = \cos \gamma_n \text{ or } \frac{V_y \cos \beta + V_H \sin \beta}{V \sqrt{x^2 + y^2 + H^2}} = \cos \gamma_n \quad (145)$$

This can be written as

$$y^2 (\cos^2 \gamma_n - \cos^2 \beta) - 2Hy \sin \beta \cos \beta + x^2 \cos^2 \gamma_n = H^2 (\sin^2 \beta - \cos^2 \gamma_n) \quad (146)$$

In order to simplify notation somewhat, let

$$\cos^2 \beta = C$$

$$\sin^2 \beta = D$$

$$\cos \beta = c$$

$$\sin \beta = d$$

Then for the general case, Equation (144) becomes

$$y^2 (\cos^2 \gamma_n - C) - 2Hydc + x^2 \cos^2 \gamma_n = H^2 (D - \cos^2 \gamma_n) \quad (147)$$

For horizontal flight, ($\beta = 0$), Equation (146) reduces to

$$(y^2) (\cos^2 \gamma_n - 1) + x^2 \cos^2 \gamma_n = -H^2 \cos^2 \gamma_n$$

or

$$x^2 + H^2 = y^2 \tan^2 \gamma_n \quad (148)$$

For a given value of (β), (γ_n), and (H), the general equation can be recognized (Farrell and Taylor, 1963) as a simple conic section, with the following possible forms

$$\beta < \gamma_n \text{ --- hyperbola} \quad (149)$$

$$\beta = \gamma_n \text{ --- parabola} \quad (150)$$

$$\beta > \gamma_n \text{ --- ellipse} \quad (151)$$

and a degenerate case when $\gamma_1 = \pi/2$ which reduces Equation (147) to the straight line

$$y = -H \tan \beta \quad (152)$$

This straight line in the x-y plane separates the regions of opening and closing doppler and is designated as the first isodop.

Since the objective is to calculate the power spectrum of the clutter return, the angle (γ_n) will be expressed in terms of the doppler frequency shift between the n^{th} and the $n + 1$ isodop. Recalling the first isodop is defined by $\gamma_1 = \pi/2$ and letting a constant, B , equal the incremental doppler shift Δf_d , the doppler shift can be expressed as

$$\Delta f_{d_{21}} = B = \frac{2V}{\lambda} (\cos \gamma_2 - \cos \gamma_1) = \frac{2V}{\lambda} \cos \gamma_2 \quad (153)$$

and

$$\Delta f_{d_{31}} = B = \frac{2V}{\lambda} (\cos \gamma_3 - \cos \gamma_2) \quad (154)$$

Then Equations (153) and (154) yield

$$\cos\gamma_2 = \frac{B\lambda}{2V} \quad (153)$$

and

$$B = \frac{2V}{\lambda} (\cos\gamma_3 - \cos\gamma_2) = \frac{2V}{\lambda} \cos\gamma_3 - B \quad (154)$$

or

$$\cos\gamma_3 = (2) \frac{\lambda B}{2V} \quad (155)$$

similarly for the n^{th} isodop

$$\cos\gamma_n = (n-1) \frac{\lambda B}{2V} \quad 1 \leq n \leq \frac{2V}{\lambda B} \quad (156)$$

The substitution of (156) in (147) changes the general equation to

$$\begin{aligned} y^2 \left[\frac{(n-1)^2 \lambda^2 B^2}{(2V)^2} - C \right] - 2HyCd + x^2 \left[\frac{(n-1)^2 \lambda^2 B^2}{(2V)^2} \right] \\ = H^2 \left[\frac{D - (n-1)^2 \lambda^2 B^2}{(2V)^2} \right] \end{aligned} \quad (157)$$

A second parameter that has a major effect on the clutter return is θ . The range to the point P in the ground plane and scattering coefficient corresponding to the area at P are a function of θ . The loci of all points in the x-y plane having the same angle of incidence is a circle defined by

$$x^2 + y^2 = H^2 \tan^2 \theta \quad (158)$$

The intersections of the sets of loci defined by Equations (157) and (158) will be used to define incremental areas for power return calculations in the following paragraphs.

Calculation of Received Power

In Section II, the power received by a pulse radar was shown to be

$$\bar{P}_r = \frac{\lambda^2}{32\pi^2} \iint P_T \left(T - \frac{2R}{C}\right) G^2(\theta, \phi) \sigma_o(\theta, \lambda) \frac{1}{R^3} dR d\phi \quad (4)$$

Now if the total ground area is divided into small incremental areas, A_n , then the power return from the n^{th} area can be expressed as

$$\bar{P}_{r_n} = \frac{\lambda^2}{(4\pi)^3 R^4} \bar{P} \left(T - \frac{2R}{C}\right) G_n^2(\theta_n, \phi_n) \sigma_o(\theta_n, \lambda) A_n \quad (159)$$

The total average power received is then

$$\bar{P}_r = \sum_{n=1}^N \bar{P}_{r_n} \quad (160)$$

where P_t , G_n^2 , and σ_o are assumed to be constant over the area A_n .

Derivation of the Incremental Area. The incremental areas can be defined by the intersections of the isodops and the circles corresponding to angles of incidence as shown in Fig. 10. The intersection of the n^{th} isodop and the n^{th} circle can be found from Equations (156) and (157) as

$$\begin{aligned} y^2 (\cos^2 \gamma_n - \cos^2 \beta) - 2Hy \sin \beta \cos \beta + x^2 \cos^2 \gamma_n \\ = H^2 (\sin^2 \beta - \cos^2 \gamma_n) \end{aligned} \quad (157)$$

and

$$x^2 + y^2 = H^2 \tan^2 \theta_n \quad (158)$$

Substitution of $x^2 = H^2 \tan^2 \theta_n - y^2$ in Equation (157) and solution for y yields

$$y_n = -H \tan \beta \pm H \sec \beta \cos \gamma_n [\tan^2 \theta_n + 1]^{1/2} \quad (161)$$

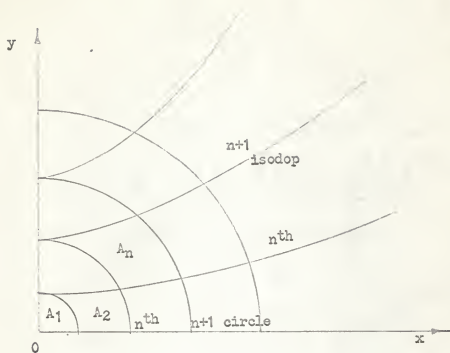


Fig. 10. Incremental areas.

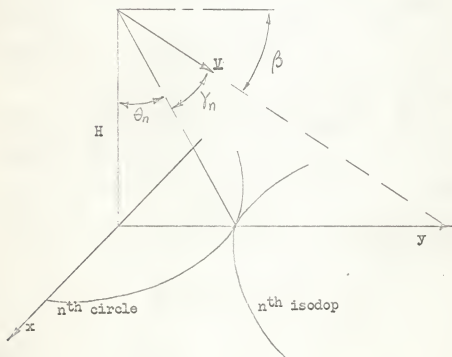


Fig. 11. Intersection of n^{th} circle and n^{th} isodop.

and

$$x_n = [H^2 \tan^2 \theta_n - y_n^2]^{\frac{1}{2}} \quad (162)$$

If the coordinates are normalized for $H = 1$, Equations (161) and (162) become

$$x_n = [\tan^2 \theta_n - y_n^2]^{\frac{1}{2}} \quad (163)$$

$$y_n = -\tan \beta \pm \sec \beta \cos \gamma_n (\tan^2 \theta_n + 1)^{\frac{1}{2}} \quad (164)$$

where x_n and y_n are the normalized coordinates of the intersection of the n^{th} circle and n^{th} isodop. The above equations are now modified, so that the desired doppler bandwidth defines the angles θ_n and γ_n . It was shown in Equation (156) that $\cos \gamma_n$ can be expressed as

$$\cos \gamma_n = (n - 1) \frac{\lambda_B}{2V} \quad (156)$$

The angle θ_n is related to γ_n as shown in Fig. 11 as

$$\theta_n = \frac{\pi}{2} - \gamma_n - \beta \quad (165)$$

The intersection of the n^{th} circle and the n^{th} isodop will always be on the y axis. This was chosen to simplify the computer program and does not limit the solution.

Antenna Gain Associated with A_n . In general, the antenna gain is a function of both θ_n and ϕ_n , which are modified forms of the pattern reference angles. For the case of a circularly symmetrical pattern (E plane and H plane beamwidths equal) the gain corresponding to a given A_n , can be determined as follows. The angle α_n is the desired antenna pattern parameter. It is a function of the lines \overline{AP} , \overline{AB} , and \overline{PB} , as shown in Fig. 12. The line \overline{PB} is determined from the angles θ_n and ϕ_n by the law of

cosines for oblique triangles. For areas in the first quadrant, V^2 is defined as

$$V^2 = F^2 + Y^2 - 2FY \cos \phi_n \quad (166)$$

where

$$F = \overline{OP} = H \tan \theta_n$$

$$Y = \overline{OB} = H/\tan \delta$$

The angle α_n is then found from the lines \overline{AB} , \overline{AP} , and \overline{PB} as

$$\cos \alpha_n = \frac{X^2 + D^2 - V^2}{2XD} \quad (167)$$

or

$$\alpha_n = \arccos \frac{X^2 + D^2 - V^2}{2XD} \quad (168)$$

where

$$D = \overline{AB} = H/\sin \delta$$

$$X = \overline{AP} = H/\cos \theta_n$$

For areas in the 2nd quadrant, the angle ϕ_n must be modified.

The interior angle is now defined as

$$Z = \pi - \theta_n$$

and the calculation of α_n is the same as before except with ϕ_n replaced by Z . The angle α_n is then used to compute the antenna gain for the given incremental area.

Scattering Coefficient. The Hayre and Moore (1962) scattering coefficients were calculated for three relative degrees of surface roughness. Figure 13 shows σ'_0 vs. θ for relatively smooth, medium rough, and very rough terrain.

Received Power. The power received from each incremental area

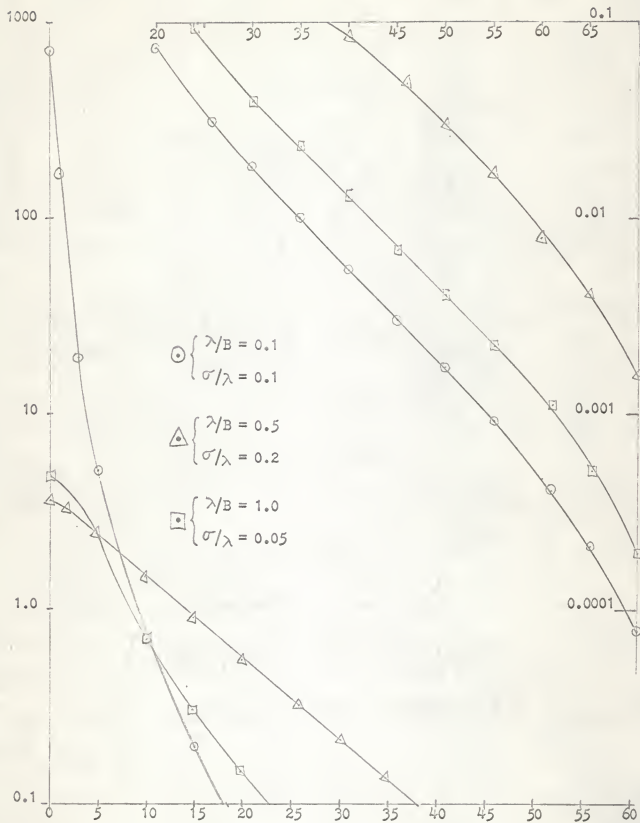


Fig. 13. Scattering coefficient (σ_0) vs. angle of incidence (θ).

is in general a function of time, and the power spectrum is time varying. The return power is nearly proportional to the illuminated area, which varies directly with the pulse width for a narrow pulse. Therefore, the average return power for a pulse-width limited return is approximately proportional to the pulse width (τ) at a fixed frequency. (Hayre and Moore, 1962). The relationship between the time of arrival, the illuminated ground area, and the angle of incidence can be derived as follows.

Assume that the average power return from the first pulse period is from range $(H + c\tau/2)$ and the return from the n^{th} pulse period is from the range $(H + (2n-1)c\tau/2)$, as shown in Fig. 14. If t_1 is the time of arrival of the first return, and t_n is the time of arrival of the n^{th} return, then

$$t_1 = \tau + 2H/c \quad (169)$$

and

$$t_n = (2n - 1)\tau + 2H/c \quad (170)$$

These returns correspond to the area in the annular ring defined by the angles of incidence, such that

$$\arccos \frac{H}{H + (n - 1)c\tau} \leq \theta \leq \arccos \frac{H}{H + nc\tau} \quad (171)$$

Thus if a time variation of the power spectrum is desired, the return is summed over the sequence of annular rings. If the average power spectrum is desired, the return is summed over the sequence of doppler bands defined by the isodops.

CALCULATED POWER SPECTRUMS

The main objective in establishing the preceding clutter model was to determine the effect of terrain roughness on the power spectrum using the Hayre-Moore (1962) scattering coefficient. Data was compiled for four scattering coefficients using the IBM 1620 digital computer.

Incremental Areas

The original program was set up for coverage out to 82.5° from the vertical. The parameters $\lambda B/2V$, Equation (156), were chosen to give 0.00877193, or approximately one-half degree increments of γ near the vertical. This resulted in 6441 incremental areas in the first quadrant for the horizontal flight condition. The program calculated the x,y coordinates of the intersections of the isodop-hyperbolas and the angle of incidence circles. Each incremental area was then approximated by the area enclosed by straight lines connecting the points of intersection. This area was calculated using the determinant solution for the area of a triangle given as (Burlington, 3rd Ed.)

$$A = \frac{1}{2} \begin{vmatrix} X_1 & Y_1 & 1 \\ X_2 & Y_2 & 1 \\ X_3 & Y_3 & 1 \end{vmatrix} = \text{Area of a triangle with vertices } (X_1, Y_1), (X_2, Y_2), (X_3, Y_3). \quad (172)$$

Equation (172) was modified to account for the two triangles making up the incremental area. The excessive Computer time necessary for the IBM 1620 to run the program for 6441 incremental areas made it impractical for the intended use. The

areas for the first three isodops were calculated by integration and compared with the computed areas. An error of approximately -3% was obtained. Computation time was about twenty minutes for these isodops using Fortran II. It was estimated that five to eight hours would be required for the total 6441 incremental area program.

The parameters were then changed to give $\lambda B/2V = 0.01745$, or approximately one degree increments of γ near the vertical, and the coverage was reduced to 73.7° . This resulted in 1540 incremental areas in the first quadrant. This program was checked for the first three isodops and for the total area in the first quadrant. The computational error was approximately -7.5% for the first three isodops, but was only -0.33% for the total area.

The modified program was then run to calculate the incremental areas weighted by $\cos^4 \theta_n$, to give the normalized ($H = 1$) range weighted areas. The values of θ_n and A_n were punched out for use as data input cards for the remaining portion of the spectrum calculations. The program parameters used for the range weighted incremental areas were $\lambda = 3.2$ centimeters, $V = 850$ feet per second (approximately 500 knots), and $B = 282.6$ cycles per second.

Scattering Coefficients

The program for the Hayre-Moore (1962) scattering coefficient was run for the following parameters:

Case #1	$\lambda/B = 0.5$	medium roughness
	$\sigma/\lambda = 0.4$	
Case #2	$\lambda/B = 0.1$	relatively smooth
	$\sigma/\lambda = 0.1$	
Case #3	$\lambda/B = 1.0$	very rough
	$\sigma/\lambda = 0.8$	

The first runs were made using ten iterations for the series term of Equation (5). This resulted in fast convergence in Case #2 only. The results for Case #1 and Case #3 were greatly in error. A modified program was run to check the value of the n^{th} term of the series. For Case #1, the value reached a maximum on the 23rd term. After the 34th term, the value was still in excess of 10^6 . For Case #3, the value was still increasing and was in excess of 10^{21} after the 24th term. In both cases, computer capacity was exceeded at these points and the program was stopped. A check for slowest convergence was initiated and found to occur for $\theta = 0$ when the scattering coefficient is of the form

$$\sigma_0 = K \sum_{n=1}^{\infty} \frac{(158(\sigma/\lambda)^2)^n}{(n-1)!n^3} \quad (173)$$

If σ/λ is greater than 0.4, the convergence is very slow. In order to reduce the computer time, different values of λ/B and σ/λ were chosen. Another set of values were selected to cover the entire range of surface roughness as

Case #1	$\lambda/B = 1.0$	medium roughness
	$\sigma/\lambda = 0.05$	
Case #2	$\lambda/B = 0.1$	relatively smooth
	$\sigma/\lambda = 0.1$	
Case #3	$\lambda/B = 0.5$	rough
	$\sigma/\lambda = 0.2$	

The increasing value of B/λ indicates increasing size of along-the-surface terrain roughness. The value σ/λ indicates the relative vertical heights (Hayre and Moore, 1962).

Antenna Pattern

It was desired to approximate a pencil beam antenna since this type would be used in many AMTI applications. The antenna pattern chosen for the comparison was of the form $(\sin x)/x$. A three degree beamwidth was chosen to simulate a pencil beam tracking antenna. Skolnik (1962) gives the expression for such a pattern as

$$E(\theta) = \frac{\sin(\pi(a/\lambda)\sin\theta)}{\pi(a/\lambda)\sin\theta} \quad (174)$$

where the angular distance between nulls adjacent to the peak is λ/a radians, and the beamwidth, as measured between the half-power points is $0.88 \lambda/a$ radian, or $51\lambda/a$ degrees. For a three degree beamwidth the expression for the pattern becomes

$$E(\theta) = \frac{\sin(\pi(51/3)\sin\theta)}{\pi(51/3)\sin\theta} \quad (175)$$

The pattern was assumed to be symmetrical about the antenna bore-sight. A depression angle was chosen as approximately 58° , which

gave a 41° increment for checking the effect of the antenna sidelobes past the main beam in the direction of flight.

Altitude and Power

The altitude was chosen arbitrarily as 20,000 feet. The shape of the spectrum is of primary interest and not the actual values, therefore, the transmitted power and all constants in the radar equation were chosen as unity. The return was summed over the isodops to give an average power spectrum.

Power Spectrum

A program for the power spectrum was written to include all parameters of the radar equation. This program calculated the power spectrum for all 56 positive doppler frequency bands and the first 30 negative doppler bands. This included all returns from the first quadrant and returns from the second quadrant out to 65° from the antenna boresight. The program was processed in Fortran II and after the first few doppler bands were calculated it became apparent that the program would require two to three hours running time. Therefore the program was changed to calculate the incremental areas weighted by the antenna gain and the altitude factors, but omitting the scattering coefficient. The incremental areas were punched out for use as input data in the final program. The running time was approximately three hours.

A final program which multiplied the incremental areas by

the appropriate scattering coefficient and summed the results over each doppler band, was then written. The inputs were the weighted incremental area cards, and the scattering coefficient cards. It required fifteen minutes running time. The power spectrum was calculated for four scattering coefficients. The previously calculated Hayre-Moore (1962) scattering coefficients were used, and an assumed constant scattering coefficient equal to 0.00316 (Grant and Yaplee, 1957) was used for comparison.

Results

The analysis gave data for power spectrums from four scattering coefficients in the form of return in 55 positive doppler frequency bands and 30 negative doppler frequency bands.

In order to evaluate the effect of the terrain roughness on the power spectrum, the smallest value from all data was chosen as the reference. A program to transform the results to decibels referenced to this value was then run. The final power spectrums are shown in Figs. 15-17 as db vs. doppler frequency. The power spectrums for the Hayre-Moore (1962) scattering coefficients are plotted with the spectrum for σ_0 equal to a constant for comparison. The spectrums all have a sharp peak at the first doppler band. This is the altitude return and shows the inverse fourth power effect of range. For all four spectrums, the width of the major peak is approximately 860 cycles per second. This return is from areas within 2° to 3° of the vertical.

For a smooth surface, (See Fig. 15) where $\lambda/B = 0.1$ and $\sigma/\lambda = 0.1$, the peak return is approximately 135 db above the majority of the remaining spectrum. This shows the effect of the strong specular components near the vertical. The amplitude of the spectrum has a decreasing slope between the peak return and the antenna main beam, showing the effect of the rapidly decreasing scattering coefficient for angles away from the vertical.

The spectrum for $\lambda/B = 0.5$ and $\sigma/\lambda = 0.2$ (See Fig. 16) very nearly parallels the spectrum for σ_0 equal to a constant. The peak value is about 110 db above the average value. There is a general 20-23 db difference between the spectrum for the computed coefficient and the one for the constant coefficient out to the antenna main beam portion of the spectrum. Beyond this, they converge as the σ_0 for the Hayre-Moore values approach the constant value. Both spectrums show a tendency to be flat in the sidelobe region.

The spectrum for $\lambda/B = 1.0$ and $\sigma/\lambda = 0.05$ (See Fig. 17) is almost the same as that for the smooth surface except for the peak value, which is about 110 db above the average value. This was to be expected since the scattering coefficient curves are very close for $\theta > 3^\circ$ (See Fig. 13).

All four spectrums have a lower amplitude in the main beam region than was expected. This was evidently the result of the antenna pattern sidelobe levels increasing at about the same gain slope that σ_0 was decreasing. Another factor was the

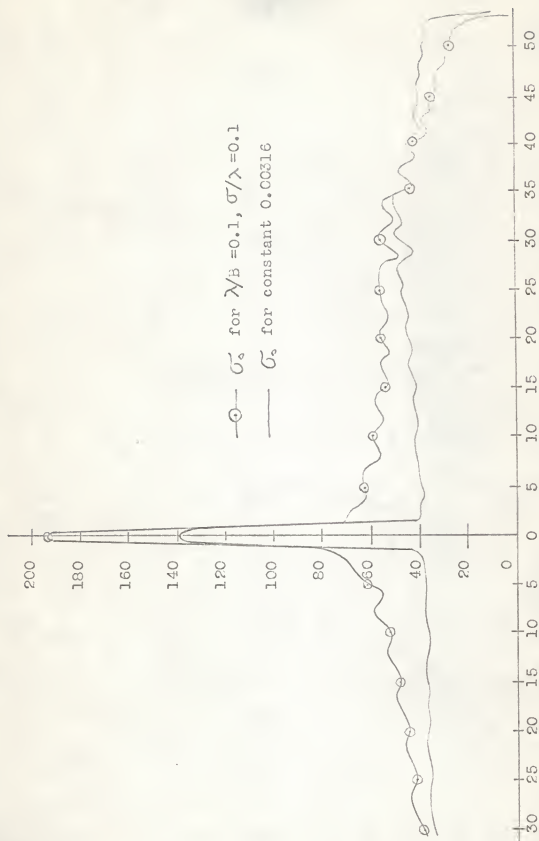


Fig. 15. Clutter spectrum in db. vs. doppler band.

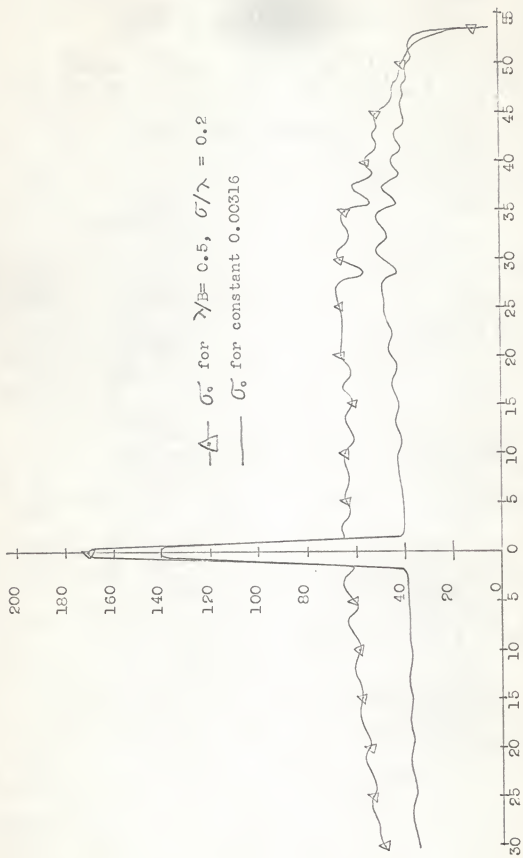


Fig. 16. Clutter spectrum in db. vs. doppler band.

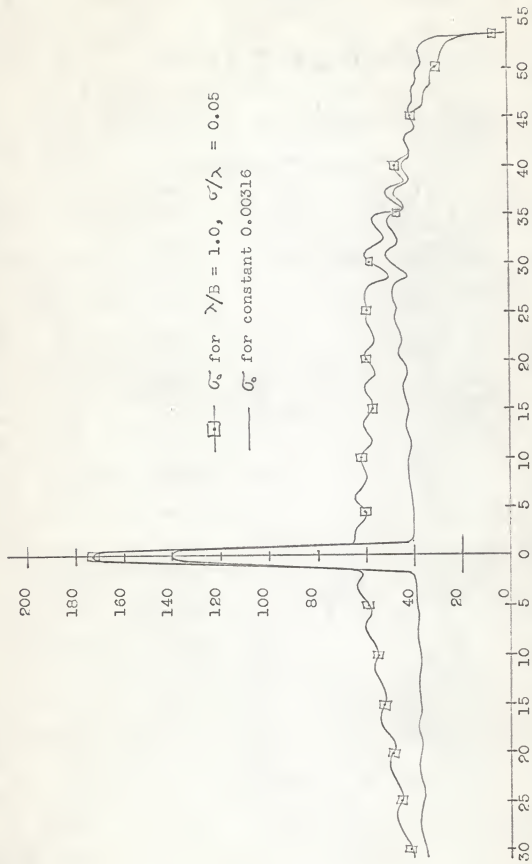


Fig. 17. Clutter Spectrum in db. vs. doppler band.

angular width of the incremental areas. These were wider than desirable because of the computing time considerations previously mentioned. This may have caused the peak of the main beam gain to have had less effect than it should have. The spectrums do, however, show that terrain roughness variations have a relatively minor effect away from the vertical (3° - 5°) angles of incidence. They also show that the assumption of σ_0 equal to a constant holds relatively well over a large portion of the spectrum, but is very pessimistic at the ends of the spectrum. This is just the portion of the spectrum which is important in evaluation of radars using doppler frequency detection techniques. The use of a constant σ_0 causes the computed power to be too high at these frequencies and will not give an accurate evaluation of the radar's capability in the critical low velocity region.

The curves for σ_0 given by Hayre and Moore (1961), those in Fig. 13, and the corresponding power spectrums seem to indicate that the value of σ/λ determines the average power level, whereas the value of λ/B determines the slope of the spectrum. This relationship needs further investigation.

SUMMARY

Airborne radar AMTI clutter models and methods of analysis are discussed. The basic radar return theory is briefly reviewed. Emphasis is placed on the Hayre-Moore (1962) scattering coefficient, which allows a quantitative expression for the effect of surface roughness on the radar return. The relation-

ship between signal correlation and power spectrum are discussed and two basic correlation receivers are diagramed.

Analyses of clutter and AMTI performance reported in the literature are reviewed. There are two general forms of analysis used, namely, random variable theory and deterministic models. Much of the effort reported in the literature has been concerned with calculation of clutter cancellation ratios and the probability of detection for radars using phase or amplitude clutter cancellation. These papers fall in the random variable theory class. In theoretical analysis, Urkowitz's assumption of a "white noise" spectrum for the clutter and Bailey's assumption of a gaussian spectrum for the clutter are commonly used. The second class of analysis is concerned with calculation of ground clutter power spectrum for given parameters. The work done by Welch at the New Mexico State University and a recent paper by Farrell and Taylor of Westinghouse are used as a basis for a modified mathematical model for calculation of ground clutter power spectrum. The major contribution of this thesis is use of the Hayre-Moore (1962) scattering coefficient for investigation of the effect of terrain roughness on the clutter spectrum.

Clutter spectrums are calculated for three Hayre-Moore (1962) scattering coefficients and an assumed constant scattering coefficient. Data was compiled using the IBM 1620 digital computer. The increments in the final modified program were slightly larger than desirable, but the program had sufficient accuracy to show the usefulness of the technique. Better results would be obtained

with smaller increments on a larger and faster computer than the IBM 1620. The effect of terrain roughness is most prominent near the vertical or for $0 < \theta < 3^\circ$. At angles greater than approximately three to four degrees, there is no major change in the shape of the spectrum as the roughness varies. A comparison of the spectrums for the Hayre-Moore (1962) scattering coefficients with that for a constant coefficient, showed that the assumption of σ_0 as a constant gives a very large error in the power spectrum at the high frequency end. This is the area of prime importance in a doppler frequency detection system, as the performance against low velocity targets is determined by the signal to clutter ratio as the signal moves into the clutter region of the spectrum.

ACKNOWLEDGMENTS

The author wishes to express his gratitude to Dr. H. S. Hayre, of the Department of Electrical Engineering, for his guidance while preparing this paper. Also special thanks are due to Dr. C. A. Halijak, Department of Electrical Engineering, for his suggestions on the area approximation; to Dr. B. D. Weathers, Department of Electrical Engineering, for his help in early computer programming problems; and to W. Hull, fellow graduate student, for his time and instruction on the IBM 1620 computer.

REFERENCES

1. Bailey, F. B.
A method for calculating the probability of detection for a coherent (AMTI) radar unit with phase cancellation. Jour. Frank. Inst. April 1963.
2. Bendat, J. B.
Principles and applications of random noise theory. John Wiley & Sons, Inc. 1958.
3. Chia, C.
Computer programs for determining radar return power and fading spectra. Master's Thesis. The University of New Mexico. 1960.
4. Coleman, S. D. and Hetrich, G. R.
Ground clutter and its calculation for airborne pulse doppler radar. IRE Conv. Rec. Mil-E-Con. June 1961.
5. Dickey, F. R. Jr.
Theoretical performance of airborne moving target indicators. IRE Trans. PGAE-8. June 1953.
6. Farrell, J. L. and Taylor, R. L.
Doppler radar clutter. Westinghouse Elec. Corp. Report No. AA-4285. July 1963.
7. Grant, C. R. and Yaplee, B. S.
Back scattering from water and land at centimeter and millimeter wavelengths. Proc. IRE. July 1957.
8. Hayre, H. S. and Moore, R. K.
Theoretical scattering coefficients for near vertical incidence from contour maps. Jour. Res., Nat. Bu. Stds. Vol. 65D. No. 5. Sept.-Oct. 1961.
9. Hayre, H. S. and Moore, R. K.
Radar back-scattering theories for near-vertical incidence and their application to an estimate of the lunar surface roughness. Dissertation for D. Sc. at The University of New Mexico. 1962.
10. Remely, W. R.
Correlation of signals having a linear delay. Jour. Acoust. Soc. of Amer. Vol. 35. No. 1. January 1963.
11. Rice, O. S.
Mathematical analysis of random noise. Bell Sys. Tech. Jour. Vol. 23 and 24. 1948.

12. Skolnik, M. I.
Introduction to radar systems. McGraw-Hill. 1962.
13. Urkowitz, H.
An extension to the theory of the performance of airborne moving target indicators. IRE Trans. on Aero. and Nav. Elect. Vol. ANE-5. December 1958.
14. Welch, P. D.
Interpretation and prediction of radar terrain return fading spectra, progress reports I, II, and III. Sandia Corporation Reprints SCR-212, SCR-214, and SCR-215. July 1960.

APPENDIX

Digital Computer Program for Incremental Areas

The problem was initially programmed for an IBM 1620 computer using FORGO. The following variables and symbols are defined for this program.

Data Input

$$B = \lambda B / 2V$$

$$U = \tan \beta$$

$$H = H^2 \text{ (altitude squared)}$$

$$D = \sec \beta$$

$$TA = \beta \text{ (radians)}$$

Program Variables

$$G = (n - 1)$$

$$W = (n - 1)$$

$$TH(I) = \theta_n$$

$$CO(I) = \cos^4(\theta_n)$$

$$Z(I) = \tan^2(\theta_n)$$

$X(1,J)$ = x coordinate of intersection of the J^{th} circle and the 1st isodop in the doppler frequency band.

$Y(1,J)$ = y coordinate of above.

$X(2,J)$ = x coordinate of the J^{th} circle and 2nd isodop in the doppler frequency band.

$Y(2,J)$ = y coordinate of above.

$PH(J) = \phi_n$, the angle between the y axis and the area $A(J)$.

$A(J) = J^{\text{th}}$ incremental area.

The program starts by calculating the γ_n corresponding to the doppler bandwidth selected. This is done by denoting γ_n as $TH(I)$ and setting $TH(1) = \pi/2$. The 1620 does not have an arccosine subroutine, therefore the angle must be found from the arctan of γ_n . The $\tan \gamma_n$ is related to the $\cos \gamma_n$ by

$$\tan \gamma = \frac{\sqrt{1 - \cos^2 \gamma_n}}{\cos \gamma_n}$$

Since, (156), $\cos \gamma_n = (n - 1)\lambda B/2v$, the calculation is:

$$TH(I) = ATAN (SQRT(1.-G*G*B*B)/(G*B))$$

where $TH(I)$ at this point is γ_n . The angle θ_n is now found from

(165) as

$$TH(I) = 1.57079633 - TH(I) - TA$$

These values are stored for future use in the power density calculations. Next $\cos^4(\theta_n)$ and $\tan^2(\theta_n)$ are calculated by

$$Z(I) = \cos (TH(I))$$

$$CO(I) = Z(I) * Z(I) * Z(I) * Z(I)$$

Where $Z(I)$ at this point is $\cos(\theta_n)$. The values for $\tan^2(\theta_n)$ are now calculated by the relationship

$$\tan^2(\theta_n) = (1/\cos^2 \theta_n) - 1$$

or

$$Z(I) = (1./(Z(I) * Z(I)) - 1.$$

The values of $CO(I)$ and $Z(I)$ are stored for future use. Next the coordinates for the points of intersection are calculated. Only one doppler band at a time will be calculated, because of

computer storage limitations. This is done by calculating $X(1,J)$, $Y(1,J)$, $X(2,J)$, and $Y(2,J)$ for the first doppler band defined by γ_1 and γ_2 . For the second doppler band defined by γ_2 and γ_3 , the coordinates $X(2,J)$ and $Y(2,J)$ become $X(1,J)$ and $Y(1,J)$. A new set of $X(2,J)$ and $Y(2,J)$ are calculated.

From Equations (163) and (164):

$$Y(1,J) = -U$$

$$X(1,J) = \text{SQRT}(Z(J) - U*U)$$

(the $\cos \gamma_1$, defining the 1st isodop is always zero.)

then

$$Y(2,1) = 0.0$$

$$X(2,1) = 0.0$$

This is necessary because in the subscripts adopted there are no $Y(2,1)$ or $X(2,1)$. Then

$$Y(2,J) = (W*B*D*\text{SQRT}(Z(J) + 1.)) - U$$

$$X(2,J) = \text{SQRT}(Z(J) - Y(2,J) * Y(2,J))$$

Next the angle ϕ_n corresponding to the incremental area A_n is calculated. The angle ϕ_n is defined as the angle between the y axis and a line from the origin to a point X_n, Y_n where

$$X_n = \frac{X(1,J) + X(2,J) + X(1,J + 1) + X(2,J + 1)}{4}$$

$$Y_n = \frac{Y(1,J) + Y(2,J) + Y(1,J + 1) + Y(2,J + 1)}{4}$$

then

$$\phi_n = \arctan (X_n/Y_n)$$

or

$$\text{PH}(J) = X(1,J) + X(2,J) + X(1,J + 1) + X(2,J + 1)$$

$$Q(J) = Y(1,J) + Y(2,J) + Y(2,J + 1) + Y(1,J + 1)$$

and

$$PH(J) = ATAN (PH(J)/Q(J))$$

The incremental area $A(J)$ is approximated by connecting the points of intersection by straight lines and finding the area enclosed by them. The solution of the area of the two triangles defined by the approximation to $A(J)$ gives

$$A(J) = X(1,J) * (Y(1,J + 1) - Y(2,J))$$

$$F(J) = X(1,J + 1) * (Y(2,J + 1) - Y(1,J))$$

$$Q(J) = X(2,J) * (Y(1,J) - Y(2,J + 1))$$

$$V(J) = X(2,J + 1) * (Y(2,J) - Y(1,J + 1))$$

$$A(J) = 0.5 * (A(J) + F(J) + Q(J) + V(J))$$

Finally the incremental areas were weighted for the normalized range by multiplying by $\cos^4 \theta_n$.

$$A(J) = A(J) * CO(J)$$

The complete program for the normalized range weighted areas follows.

```

C      INCREMENTAL RANGE WEIGHTED AREAS FOR POWER SPECTRUM
      READ 101,U,B,H, D,TA
101  FORMAT(F3.1,2X,F9.9,2X,F3.1,2X,F3.1,2X,F3.1)
      DIMENSION CC(56),Z(56),F(56),Q(56),V(56)
      DIMENSION X(2,56), Y(2,56), A(55),TH(56), PH(56)
      TH(1)=1.57079633
      DC 1 I=2,56
      G=I-1
1  TH(I)= ATAN((SQRT(1.-G*G*B*B))/(G*B))
      DC2 I=1,56
      TH(I)=1.57079633-TH(I)-TA
      Z(I) = COS(TH(I))
      CC(I)= Z(I)*Z(I)*Z(I)*Z(I)
2  Z(I)=(1./(Z(I)*Z(I)))-1.
      DC3 J=1,56
      X(1,J)=0.0
      Y(1,J)=0.0
      X(2,J)=0.0
3  Y(2,J)=0.0
      M=52
      L=51
      W=M-1
4  DC5 J=M,56
5  Y(2,J)=(W*B*D*SQRT(Z(J)+1.))-U
      X(2,M)=0.
      M=M+1
      IF(M-57)10,11,30
10  DC9 J=M,56
9  X(2,J)=SQRT(Z(J)-(Y(2,J)*Y(2,J)))-U
11  DC6 J=L,55
      PH(J)=X(1,J)+X(1,J+1)+X(2,J)+X(2,J+1)
      Q(J)= Y(1,J)+Y(1,J+1)+Y(2,J)+Y(2,J+1)
      PH(J)=ATAN(PH(J)/Q(J))
      A(J)= X(1,J)*(Y(1,J+1)-Y(2,J))
      F(J)= X(1,J+1)*(Y(2,J+1)-Y(1,J))
      Q(J)= X(2,J)*(Y(1,J)-Y(2,J+1))
      V(J)= X(2,J+1)*(Y(2,J)-Y(1,J+1))
      A(J)= .5*(A(J)+F(J)+Q(J)+V(J))
6  A(J)=A(J)*CC(J)
      DC7 J=L,55
7  PUNCH 17, A(J), L,J
17  FORMAT(E15.8,10X,I3,2X,I3)
      DC8 J=L,55
8  PUNCH 17, PH(J), L,J
      DC23 J=1,56
      X(1,J)=X(2,J)
23  Y(1,J)=Y(2,J)
      N=M-1
      DC24 J=1,N
      X(2,N)=0.
24  Y(2,N)=0.
      L=L+1
      W=M-1
      IF(M-57)14,4,30
30  CONTINUE
      END

```

Computer Program for Scattering Coefficient

The scattering coefficient was calculated from Equation (5) for angles θ_n associated with the incremental areas.

Data Input

$$B = B \text{ from area program (0.01745)}$$

$$D = \sigma/\lambda$$

$$A = \lambda/B$$

Program Variables

$$TH(I) = \theta_n$$

$$H(J) = \sin \theta_n$$

$$SI(J) = \sin^2 \theta_n$$

$$CO(J) = \cos^2 \theta_n$$

$$U = B^2/\lambda^2$$

$$F = (2\pi)^2$$

$$G = 4\sqrt{2} \frac{\pi B^2}{\lambda^2}$$

$$P = 4k^2 \sigma^2 = 4(2\pi)^2 \frac{\sigma^2}{\lambda^2}$$

$$Q(J) = 4\sqrt{2} \frac{\pi B^2}{\lambda^2} \left(\frac{\theta_n}{\sin \theta_n} \right) \exp(-4k^2 \sigma^2 \cos^2 \theta_n)$$

$$X = X * (T - 1.) = (n - 1)!$$

$$R = \sum_{n=2}^{15} \frac{(4k^2 \sigma^2)^n (\cos^2 \theta_n)^{n+1}}{(n-1)! (2k^2 B^2 \sin^2 \theta_n + n^2)^{3/2}}$$

$$Y = \frac{(4k^2 \sigma^2) (\cos^2 \theta_n)^2}{(2k^2 B^2 \sin^2 \theta_n + 1)^{3/2}}$$

$$\theta(J) = \sigma_0(\theta_n)$$

First the program calculates the angles θ_n in the same way as for the incremental area program. This simplifies the final program, in that the scattering coefficient is calculated for the same angles of incidence as the areas, and no interpolation is required. Next the program constants are calculated as

$$U = (1/A) ** 2$$

$$F = 4. * 3.141593 * 3.141593 * U$$

$$G = 5.656856 * 3.141593 * U$$

$$P = 4. * F * D * D$$

Next the parameters involving $\sin \theta_n$ and $\cos \theta_n$ are calculated for all θ_n and stored.

$$CO(J) = \text{COS}(\text{TH}(J)) * \text{COS}(\text{TH}(J))$$

$$H(J) = \text{SIN}(\text{TH}(J))$$

$$SI(J) = H(J) * H(J)$$

Next the values for $Q(J)$ are calculated for all θ_n . Because $Q(J)$ has a term $(\theta_n / \sin \theta_n)$, $Q(1)$ for $\theta_1 = 0$ must be calculated separately.

$$Q(1) = G * \text{EXP}(-P)$$

$$Q(J) = G * (\text{TH}(J) / H(J)) * \text{EXP}(-P * CO(J))$$

Next the summation portion of the equation is calculated for $n = 1$ to 15. For $n = 1$, $(n - 1)! = 0! = 1$. This term is calculated separately as

$$Y = (P * CO(J) * CO(J)) / \text{SQRT}((2. * F * U * SI(SI(J) + 1.)) ** 3)$$

Next the $(n - 1)!$ term is calculated by

$$X = 1.$$

$$I = 2,15$$

$$T = I$$

$$X = X * (T - 1.)$$

The remaining terms $n = 2,15$ are then calculated as

$$R = ((P^{**T}) * (CO(J)^{**T+1.})) / (SQRT((2.*F*U*SI(J) + (T**T))^{**3}) * X)$$

$$Y = Y + R$$

Next the value of the scattering coefficient for a given θ_n is calculated and punched out as

$$O(J) = Q(J) * Y$$

PUNCH 9, O(J), TH(J), J

The complete program follows:

```

C      SCATTERING COEFFIC FOR POWER SPRECTRUM
      DIMENSION TH(56),SI(56),C(56),Q(56),O(56),H(56)
      READ40,A,D
40  FORMAT(F3.1,2X,F3.1)
      U=(1./A)**2
      F=4.*3.141593*3.141593
      G=5.656856*3.141593*U
      B=.01745
      P=4.*F*D*D
      TH(1)=1.57079633
      DC 2 I=2,56
      C=I-1
2  TH(I)= ATAN((SQRT(1.-C*C*B*B))/(C*B))
      DC 8 I=1,56
8  TH(I)=1.57079633-TH(I)
      DC3 J=1,56
      C(J)=COS(TH(J))*COS(TH(J))
      H(J)=SIN(TH(J))
3  SI(J)=H(J)*H(J)
      Q(1)=G*EXP(-P)
      DC4 J=2,56
4  Q(J)=G*(TH(J)/H(J))*EXP(-P*C(J))
      DC5 J=1,56
      Y=(P*C(J)*C(J))/SQRT((2.*F*U* SI(J)+1. )**3)
      X=1.
      DC 10 I=2,15
      T=I
      X=X*(T-1.)
      R=((P+T)*(C(J)**(T+1.)))/(X*SQRT((2.*F*U*SI(J)+(T*T)**3))
10  Y=Y+R
      O(J)=Q(J)*Y
5  PUNCH 9, O(J), TH(J), J
9  FORMAT(E15.8,4X,E15.8,30X,12)
      END

```

Computer Program for Gain and Altitude Weighted Areas

Data Input

N = doppler isodop being calculated

B = .01745 (Same as previous programs.)

H = Altitude = 20,000 feet

Y = $H/\tan\beta = H/1.6276$

D = $H/\sin\beta = H/.85203$

Program Variables

TH(I) = θ_n

F(I) = $H \tan \theta_n$

A(I) = range weighted incremental area

PH(I) = ϕ_n

$\Omega = \alpha_n$ (antenna pattern angle)

G = (gain)²

BIG(I) = positive doppler incremental areas

SIG(I) = negative doppler incremental areas

The program starts by reading in the initial value of N.

This is done so that the program can be run in segments if desired.

READ 50, N

50 FORMAT (I2)

Next B, H, Y, and D are entered and then TH(I) is calculated for all θ_n as in the previous programs. In addition F(I) is calculated for all θ_n as:

$F(I) = H * \sin(TH(I))/\cos(TH(I))$

Next the values for A(I) and PH(I) are read in for the Nth isodop.

```
READ 1, (A(I), I = N,55)
```

```
READ 1, (PH(I), I = N,55)
```

Next the corresponding antenna gain factor is calculated for each incremental area in the Nth isodop. The incremental area A₁ is a special case in which $\theta_1 = 0$ and the antenna pattern angle must be read in rather than calculated. This is done by:

```
IF(I - 1)30, 30, 35
```

```
30 Q = 0.55079633
```

```
Go to 36
```

```
35 V = SQRT((F(I)*F(I))+(Y*Y)-2.*F(I)*Y*COS(PH(I)))
```

```
X = H/COS(TH(I))
```

```
W = ((X*X)+(D*D)-(V*V))/(2.*X*D)
```

```
Q = ATAN((SQRT(1.-W*W))/W)
```

```
36 Q = 3.141593 * (51./3.) * SIN(Q)
```

```
IF(Q-Q.) 6,5,6
```

```
5 G = 1.
```

```
GO TO 7
```

```
6 G = (SIN(Q)/Q)**2
```

Next each incremental area is multiplied by the gain factor and altitude as:

```
7 BIG(I) = (A(I)*G)/(H*H)
```

Next the gain factors for the negative doppler isodops are calculated by:

```
Z = 3.141593 - PH(I)
```

The remainder of the program for the gain is the same as above except, $PH(I)$ is replaced by Z . The complete program is as follows.

```

C   ALTITUDE AND GAIN WEIGHTED AREAS
    DIMENSION A(55),PH (55),TH(56),F(56),SIG(55),BIG(55)
    READ50,N
50  FORMAT(12)
    B=.01745
    H= 20000.
    Y=H/1.6276
    D=H/.85203
    TH(1)=1.57079633
    DC 2 I=2,56
    C=I-1
    2 TH(I)= ATAN((SQRT(1.-C*C*B*B))/(C*B))
    DC 3 I=1,56
    TH(I)=1.57079633-TH(I)
    3 F(I)=H*SIN(TH(I))/COS(TH(I))
    1 FORMAT (E15.8)
    4 READ 1,(A(I),I=N,55)
    READ 1,(PH(I),I=N,55)
    DC22 I=N,55
    IF(I-1) 30,30,35
30  Q=0.55079633
    GOTO 36
35  V=SQRT((F(I)*F(I)) +(Y*Y)-2.*F(I)*Y*CCS(PH(I)))
    X=H/COS(TH(I))
    W=((X*X)+(D*D)-(V*V))/(2.*X*D)
    Q=ATAN((SQRT(1.-W*W))/W)
36  Q=3.141593*(51./3.)*SIN(Q)
    IF(Q-0.)16,5,6
    5 G=1.
    GO TO 7
    6 G=(SIN(Q)/Q)**2
    7 BIG(I)=(A(I)*G)/(H*H)
    Z=3.141593-PH(I)
    IF(I-1)31,31,37
31  Q=0.55079633
    GO TO 38
37  IF(N-30)8,8,22
    8 V=SQRT((F(I)*F(I)) +(Y*Y)-2.*F(I)*Y*CCS(Z))
    W=((X*X)+(D*D)-(V*V))/(2.*X*D)
    Q=ATAN((SQRT(1.-W*W))/W)
38  Q=3.141593*(51./3.)*SIN(Q)
    IF(Q-0.)10,9,10
    9 G=1.
    GO TO 22
10  G=(SIN(Q)/Q)**2
    SIG(I)= (A(I)*G)/(H*H)
22  CONTINUE
    DC 40 I=N,55
40  PUNCH17, BIG(I),N,I
17  FORMAT(E15.8,10X,I3,2X,I3)
    IF(N-30)29,29,25
29  DC41 I=N,55
41  PUNCH17, SIG(I),N,I
25  CONTINUE
    N=N+1
    GO TO 4
    END

```

Computer Program for Final Power Spectrum

The program for the final power spectrum reads in data cards from the programs for weighted incremental areas and scattering coefficients. This data is multiplied and summed over each isodop for the final spectrum. The complete program is as follows:

```
C      FINAL POWER SPECTRUM
      DIMENSION A(55),SIG(55), B(55)
1  FORMAT(E15.8)
      READ1,(SIG(I),I=1,55)
      N=1
4  READ1,(A(I),I=N,55)
      CWER=0.0
      PCWER=0.0
      DC5 I=N,55
5  POWER= POWER+A(I)*SIG(I)
      IF(N-30)6,6,7
6  READ1,(B(I),I=N,55)
      DC8 I=N,55
8  CWER =CWER+B(I)*SIG(I)
      PUNCH24,N,CWER
24 FORMAT(5HPOWER(,I2,3H)= E15.8)
7  PUNCH23,N,PCWER
23 FORMAT(6HPOWER(,I2,3H)= E15.8)
      N=N+1
      GO TO 4
      END
```

Computer Program for Normalized Spectrum

Data Input

X = reference power level

POWER(I) = data from power spectrum program

OWER(I) = data from power spectrum program

Program Variables

C = $\ln 10.0$

Y(I) = POWER(I)/X

DB(I) = $\frac{10 \ln(Y(I))}{\ln 10}$ = decibels

The program divides all input power levels by the reference level and then calculates the corresponding db value. These values are then punched out in the same format as before.

The complete program is as follows:

```
C      NORMALIZE POWER SPECTRUM
      DIMENSION POWER(55),CWER(30),Y(55),DB(55)
      READ2,X
2     FORMAT(E15.8)
      READ1,(POWER(I),I=1,54)
1     FORMAT(11X,E15.8)
      C=LOG(10.)
      DO3 I=1,54
      Y(I)=POWER(I)/X
      DB(I)=10.*(1./C)*LOG(Y(I))
3     PUNCH5,I,DB(I)
5     FORMAT(6HPPOWER(,I2,3H)= E15.8)
      READ6,(CWER(I),I=1,30)
6     FORMAT(10X,E15.8)
      DO7 I=1,30
      Y(I)= CWER(I)/X
      DB(I)=10.*(1./C)*LOG(Y(I))
7     PUNCH8,I,DB(I)
8     FORMAT(5HCWER(,I2,3H)= E15.8)
      END
```

AIRBORNE RADAR GROUND CLUTTER
RETURN

by

ROBERT A. McMILLEN

B. S., Kansas State University, 1960

AN ABSTRACT OF A MASTER'S THESIS

submitted in partial fulfillment of the

requirements for the degree

MASTER OF SCIENCE

Department of Electrical Engineering

KANSAS STATE UNIVERSITY
Manhattan, Kansas

1964

In analysis and design of airborne moving target indication (AMTI) radars, it is necessary to establish an accurate model for return from the ground, commonly called "clutter". This paper investigates the effect of surface roughness on clutter power spectrum. A review of the basic radar return theory with emphasis on a scattering coefficient derived by Hayre and Moore is given. This coefficient incorporates a quantitative expression for the effect of surface roughness on radar return. Signal correlation and power spectrum for random processes are also briefly reviewed.

Analyses of clutter and AMTI performance reported in the literature are included. These analyses techniques may be divided in two classes, namely, random variable models and deterministic models. Random variable models have been used extensively to calculate clutter cancellation ratios and the probability of detection for AMTI radars. Deterministic models have been used for calculation of the return power spectrum for specified parameters. A deterministic approach of Welch and recently of Farrell and Taylor was used as a basis for a modified mathematical model for the calculation of ground clutter power spectrum. The major contribution of this work is the use of the Hayre-Moore scattering coefficient for investigation of the effect of terrain roughness on the clutter spectrum.

Clutter spectrums were calculated for three varying degrees of surface roughness using Hayre-Moore scattering coefficients and for an assumed constant scattering coefficient. Data was

compiled, using an IBM 1620 digital computer, from the appended programs. Effect of terrain roughness on clutter spectrum was found to be most significant near the vertical. At angles greater than approximately three to four degrees, the shape of the spectrum is relatively insensitive to changes in surface roughness. It was found that the use of a constant scattering coefficient, as is often done in practice, may result a large error in the power spectrum at the high frequency end. This is the area of prime importance in a doppler frequency detection system, because AMTI performance against low velocity targets is primarily determined by signal to clutter ratio as the signal moves into the clutter region of the spectrum.